Heteromeric interactions between wild-type and mutant subunits of the *ether-a-go-go* related gene (hERG) channel, in the context of the type II congenital Long QT syndrome

Tianci Wang

Department of Physiology

McGill University

Montreal, Canada

April 2020

A thesis submitted to McGill University in partial fulfillment of the requirements of the degree of Master of Science in Physiology

© Tianci Wang, 2020

# **Table of Contents**

Abstract (English)	3
Abstract (Français)	5
Acknowledgements	7
Introduction	
<ol> <li>LQT syndrome</li> <li>1.1 LQTS characterization, prevalence, cause, diagnosis and treatment</li> </ol>	
<ul><li>1.2 Molecular mechanism of the congenital LQTS and the role of hERG in LQ</li><li>2. The human <i>ether-a-go-go</i> Related Gene.</li></ul>	QT2 9
2.1 hERG, Kv11.1 channel and IKr	
2.2 Isoforms of hERG	15
2.3 Structural domains of hERG  Transmembrane domains: the voltage sensor and the channel pore -	17
The cytosolic N-terminus and the PAS domain	
The cytosolic C-terminus and the CNBHD	
2.4 hERG synthesis, trafficking, and degradation	
Trafficking	
Folding	
Tetrameric assembly  Quality control and degradation	
3. Mutations of hERG	30
3.1 Types of hERG mutants	34
3.2 Dominant negative (DN) vs. Haploinsufficiency (HI) mechanism	
3.3 hERG mutants in the context of WT-mutant hetero-tetramerization	
Rationale and Objectives	41
Results	42
Expression system and mutant selections	42
Effects of hERG mutants on maturation of hERG WT	
Interaction of mutant and WT subunits	55
Discussions	61
Material and Methods	65
Reference	

#### **Abstract**

Mutations in the human *Ether-a-go-go*-Related Gene (hERG1, or KCNH2) are linked to the type 2 congenital Long QT syndrome (LQT2), characterized by delayed ventricular repolarization and predispositions for the lethal *torsade de pointes* arrhythmia. hERG1 encodes subunits of the tetrameric voltage gated potassium ion channel hERG, which controls repolarization of the cardiomyocyte plasma membrane. Among the hERG LQT2 mutations, around 88% cause trafficking defects which lead to reduced cell surface channel expression and delayed repolarization.

There are nearly 500 mutants found in hERG, but only a small fraction have been characterized. Patients are typically heterozygous, with the mutant allele overriding the function of the wild type (WT) allele. In multimeric channels like hERG, mutant subunits may exert a dominant negative (DN) effect by co-assembling with WT subunits and inducing degradation of the mixed tetramer. Alternatively, the mutant subunits may fail to interact with WT and be degraded as homotetramers or monomers, causing an overall shortage of functional subunits due to haploinsufficiency (HI). DN mutants are predicted to be more deleterious due to a greater suppressive effect on the WT subunits. This study explores the molecular mechanism of several hERG trafficking deficient mutants by detecting and distinguishing DN and HI effects. It also serves as a first step towards predicting severity of mutation phenotype based on their domain location, and assembly dynamics with WT subunits.

Constructs for differentially tagged WT hERG, and LQT2 mutants (G306W, A561V, G601S, F805C, G816V) were co-expressed in HeLa cells. Expression levels and physical association between WT and mutant hERG were assessed with immunoblot and co-immunoprecipitation experiments. Significant decreases in the levels of the mature post-Golgi

fraction of WT hERG was detected when it was co-expressed with G601S and A561V mutants, suggesting a DN effect. In contrast, no changes in WT were observed for mutants G306W, F805C and G816V, suggesting an HI effect. Strong physical association were observed between WT and G306W, A561V, and G601S mutants, consistent with DN mechanisms. Reduced interactions, and minimal post-Golgi interactions was observed between hERG WT and either F805C or G816V, suggesting an HI mechanism. Overall, this work establishes an effective experimental approach to assess hERG WT-mutant heteromers and suggests that G601S and A561V are DN mutants whereas F805C and G816V are HI mutants.

## Résumé

Les mutations dans le gène humain ether-a-go-go-related (hERG1) entrainent le syndrome du QT long congénital de type 2, caractérisé par une repolarisation ventriculaire retardée et des prédispositions aux torsades de pointes, une arythmie mortelle. hERG1 code pour les sous-unités alpha constituant le canal tétramérique potassique voltage-dépendant hERG à la membrane plasmique. 80% des mutations de hERG implique des défauts de trafic, entrainant la réduction de l'expression membranaire du canal.

Le LQT2 congénital est une pathologie de transmission autosomique dominante, ou les allèles mutants l'emportent sur la fonction sauvage. Puisque hERG est un tétramère, il est possible que les sous-unités mutées exercent un effet dominant négatif (DN) en s'assemblant avec les sous-unités sauvages, entrainant ainsi la dégradation du complexe hétérométrique. Un mécanisme d'haploinsuffisance (HI) pourrait également mener à la dégradation des sous-unités mutantes sans affecter les sous-unités sauvages, ayant pour résultat une diminution de 50% de l'expression du canal fonctionnel. Les effets DN devraient être plus sévères que l'HI, et prédire la sévérité de la pathologie en se basant sur la localisation des mutations dans la structure du canal hERG serait d'un grand intérêt. Dans ce projet, le mécanisme sous-jacent au LQT2 a été étudié en détectant et distinguant les effets DN et d'HI des mutants hERG.

Des vecteurs d'expression de hERG sauvage (hERG WT) et de mutants LQT2 (G306W, A561V, G601S, F805C, or G816V), présentant différents tags, ont été coexprimés dans des cellules HeLa, puis le niveau d'expression protéique sauvage ou mutant a été détecté par immunoblots. Avec les mutants G601S et A561V, une diminution significative de la fraction postgolgienne mature de hERG WT a été observée, suggérant un effet DN. Au contraire, aucun changement n'a été observé avec les mutants G306W, F805C et G816V, ce qui est en faveur d'un

effet d'HI. Dans un second temps, les interactions physiques entre les sous-unités sauvages ou mutantes ont étudiées par co-immunoprécipitation. Une augmentation significative de l'association physique entre la protéine sauvage et les mutants G306W, A561V et G601S a été mise en évidence, à l'inverse des mutants F805C et G816V, qui ne présentent aucune association avec la forme mature sauvage, mettant en avant un mécanisme d'HI.

Cette étude met en évidence un système expérimental permettant l'étude des interactions dynamiques entre hERG WT et les mutants hERG, avec des résultats préliminaires sur les mutants G601S et A561V qui entraineraient un effet DN et les mutants F805C et G816V un effet d'HI. Ainsi, une analyse méthodique des différents mutants de hERG peut maintenant être conduite.

# Acknowledgement

First and foremost, I'd like to express my deep appreciation for my supervisors Dr. Alvin Shrier and Dr. Jason Young. Thank you Al for trusting me with the opportunity to work in your lab and on this project. You are an incredible boss, always supportive and excited about new project directions. Moreover, I learned immensely about optimism, resilience, and passion for this field, from witnessing you succeeding at patch clamp again. Jason, thank you for patiently guiding me through this journey. You taught me to think critically and logically. You also taught me discipline, strategies to calmly approach a complicated problem or situation, as well as setting up plan and expectations rationally. What I learned from you have helped me immensely in other areas of life too.

To my committee members Dr. Terry Hebert, Dr. John Hanrahan, and D. Ursula Stochaj, thank you for your valuable time, useful insights and constructive criticisms on my project.

I'd like to thank all members of the Shrier and Young lab for their support. Special thanks to Michael Wong and Brittany Williamson for their training, guidance and mentorship. Special thanks to Dr. Camille Barbier for always being so extremely helpful and caring, and for translating my abstract. Special thanks to Kevin Guo for being my confidant in the lab, and for all the deep discussions about hERG, ERAD, life, and haunted videos. Also special thanks to Annie Boucher, Dr. Alina Ilie and Rebecca Flessner for their repeated help in managing labs duties, and for generously sharing their equipment, reagents and protocols.

Lastly, I'd like to thank my parents and my boyfriend Frank for their unconditional in trust and support, and for coming to Montreal to keep me accompanied during stressful times.

Thank you mom for being my role model, I'm eternally grateful for you.

# **Introduction**

# 1. Long QT syndrome (LQTS)

# 1.1 LQTS characterization, prevalence, cause, diagnosis and treatment

Long QT syndrome (LQTS) is a potentially lethal cardiac condition, named after its distinctive 12-lead electrocardiogram (ECG) pattern (Figure 1A) (1). The QT interval is measured from the beginning of the QRS complex to the end of the T wave, and a long QT interval reflects a prolonged duration of ventricular depolarization (QRS) and/or repolarization (T wave). This ECG abnormality is potentially dangerous, as it can develop into polymorphic ventricular tachycardia torsade de pointes (Figure 1A), which may then deteriorate into ventricular fibrillation and cardiac arrest. LQTS can be congenital or acquired. According to a 2007 ECG and genetic screening of 44,596 neonates, the prevalence of congenital LQTS is estimated to be about 1 in 2,000 live births (2-5). Acquired LQTS can be induced by many drugs, including antiarrhythmics and psychotropic agents, through the off-target blockade of the cardiac potassium channel Kv11.1 (hERG) (2,6-8). In fact, drug induced LQTS has become a major safety concern in the process of drug development, and Kv11.1 block screening is required before a newly developed drug enters the clinical phase (9). In addition, LQTS can also result from electrolyte disturbances, such as hypokalemia, hypomagnesemia and hypocalcemia (6). LQTS can also occur secondary to a pre-existing condition or risk factor that compromises heart function, such as hypothyroidism, congestive heart failure, left ventricular hypertrophy, and early stages of cardiac ischemia (6,10,11).

LQTS is typically diagnosed through its two cardinal manifestations, recurrent syncopal episodes with or without cardiac arrest, and ECG abnormalities (4). Cardiac events in LQTS patients can be triggered by acute cardiac stress, such as fatigue, strenuous exercise, sudden

noise/visual stimuli or emotional distress. Nevertheless, they may also occur during rest or during ordinary daily events (2,12). On the 12-lead ECG, LQTS is defined as having a corrected QT interval of greater than 488 ms, compared to a typical range of 400-440ms; it may also be accompanied by T wave abnormalities, such as biphasic or notched T waves (3,4). Due to the intrinsic variability of the QT interval and clinical presentation between individuals, family history is also factored into consideration. Patients with family history of syncope or sudden death in adults <40 years old have a high likelihood of suffering from LQTS (2,3,10).

Following a positive LQTS diagnosis, there are a few available treatment options. The first line of treatment is β-adrenergic receptor blockade (β-blockers), which broadly decreases the risks of stress-related cardiac events through inhibiting receptors in the sympathetic nervous system (2,13). For patients with recurrent symptoms despite β-blocker treatment, other options include implantable cardioverter-defibrillator (ICD) and left cardiac sympathetic denervation (LCSD). ICD is a device that is surgically implanted into the patient's chest to monitor cardiac dynamics. If an abnormal rhythm is detected, it automatically delivers electric shocks to convert the heart back to a normal sinus rhythm (2,10). LCSD involves the surgical ablation of specific sympathetic nerves and satellite ganglions, thus decreasing norepinephrine release at the ventricle (2,10). All these currently available treatments are limited, as they either require lifelong strict medication compliance or are invasive and can potentially impose significant complications. More importantly, none of these treatments are directly targeted for treating LQTS. Therefore, further fundamental research is needed towards the understanding of cardiac channelopathies, in order to optimize strategies of LQTS diagnosis and treatment.

# 1.2 Molecular mechanism of the congenital LQTS and the role of hERG in LQT2.

Cardiomyocytes are basic functional units of the ventricles. Individual cardiomyocytes are inter-connected via gap junctions, which allow the direct passage of intracellular ions and electrical impulses between cells. This connectivity allows cardiomyocytes to contract in a synchronized fashion, pumping blood into the systemic and pulmonary circulations. Cardiac contractions are elicited and controlled by the cardiac action potential, which consists of cyclical changes in membrane electrical potential, mediated by ionic currents flowing across the plasma membrane of cardiomyocytes dynamically (14). The mammalian ventricular action potential is divided into 5 phases (Figure 1B). Phase 0 is the initial membrane depolarization, due to the rapid influx of Na+ mediated by inward sodium current I<sub>Na</sub>. By convention, an inward current is defined as cations moving into the cells, which promotes depolarization of the plasma membrane. The initial depolarization is followed by a brief repolarization during phase 1, which is due to the fast-transient outward potassium current Ito. This is followed by phase 2, referred to as the plateau phase, during which membrane potential is sustained at a depolarized state. This is a result from the balancing of the calcium influx from the L type Ca<sub>2+</sub> current (IC<sub>a</sub>L) and the potassium efflux via two outward delayed rectifier potassium currents Ikr (rapid) and Iks (slow) (14,15). The plateau phase ceases, and phase 3 repolarization begins as ICaL inactivates, while the two potassium currents persist. This results in the repolarization of the membrane to the resting state of -85mV (phase 4), and is maintained by the inward rectifier current Iki (14,15). The Na<sub>+</sub>/K<sub>+</sub> pump plays a key role in restoring the electrolytic balance of the cardiomyocytes following an action potential by exporting Na+ and importing K+, with the energy harnessed from ATP hydrolysis (14,15).

Up to date, there are 16 genes identified that are related to congenital LQTS, all of which encode cardiac ion channel subunits or modulators involved in the ventricular action potential (4,10). Three genes KCNQ1, KCNH2, and SCN5A account for the majority of cases, making them the most prevalent subtypes (3,4,14). Among them, Long QT syndrome type 2 (LQT2) represents about 35-40% of the genotyped LQTS patients. It results from mutations in hERG (human Ether-a-go-go Related Gene, or KCNH2), which encodes the Kv11.1 channel protein, that comprises the  $\alpha$ -subunits (pore) of the potassium channel underlying the IK<sub>r</sub> current (3,4,14). Should Ikr be compromised, phase 3 of the action potential will be prolonged and cardiac repolarization phase will be delayed. Importantly, this predisposes the heart to early afterdepolarizations (EADs), where further depolarization occurs during the plateau phase of the action potential, or delayed afterdepolarizations (DADs) (Figure 1C), where an action potential to be elicited prematurely. These abnormalities may further degenerate into *Torsade de pointes*, the characteristic, and often lethal arrythmia observed in LQT2 patients. Of note, hERG is a frequently blocked as an off-target effects of many clinically successful drugs on the market, making it the major mechanism of acquired LQTS, and expanding its role in overall LQTS pathologies (16).

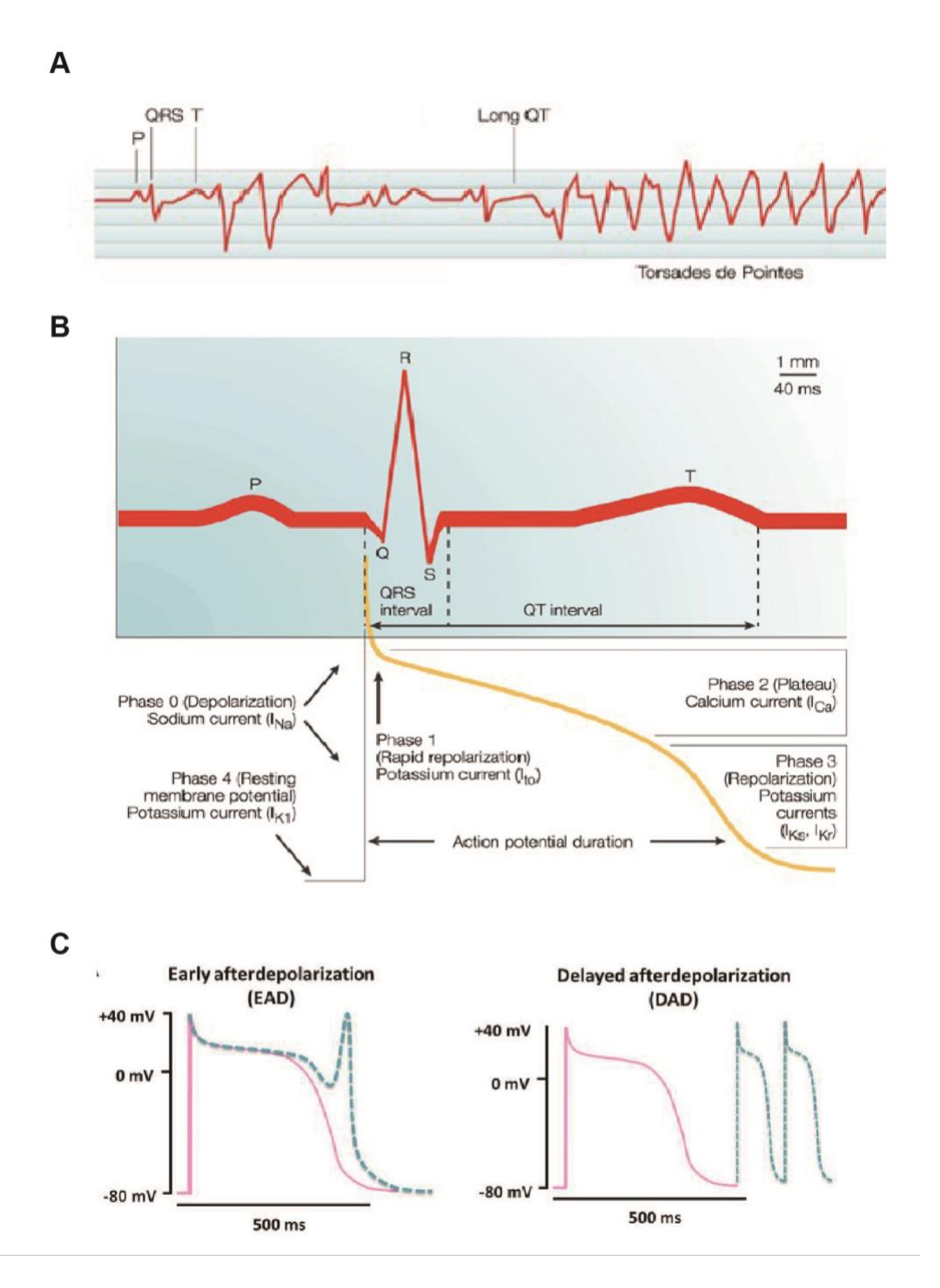


Figure 1: ECG pattern of LQT syndrome; ventricular action potential; early afterdepolarization and delayed afterdepolarization. A: ECG pattern showing a normal sinus rhythm, prolonged QT interval, and torsade de pointes arrythmia. Figure obtained from (17). B: Surface ECG (red, top) is a reflection of ventricular action potential (yellow), ionic currents shaping the

action potential are indicated by black arrows, figure obtained from (17). C: Action potentials triggered by early afterdepolarizations (EAD) and delayed afterdepolarizations (DAD) (dashed line, blue), figure obtained from (18).

# 2. The human Ether-a-go-go Related Gene.

## 2.1 hERG, Kv11.1 channel and Ikr.

The human Ether-a-go-go Related Gene (hERG, gene name KCNH2) encodes the ion channel protein that underlies  $I_{Kr}$  current in the cardiomyocyte. The channel protein is commonly referred to as hERG, while the channel is called Kv11.1, or hERG channel, used interchangeably. However, Kv11.1/hERG also refers to the ion channel that is expressed in heterologous systems, which is comprised of only the  $\alpha$  pore forming subunits underlying the naturally occurring  $I_{Kr}$  channel in the cardiomyocytes (19).  $I_{Kr}$  may also involve  $\beta$ -subunits, which are accessory subunits that regulate its function in a direct or indirect manner. KCNE1 and KCNE2 are single transmembrane domain proteins that have been proposed to act as  $\beta$ -subunits of  $I_{Kr}$ . Studies have shown evidence of them associating with hERG and alter its gating kinetics in mammalian cell lines (3,4,19-23).

hERG channel is a voltage-gated, rapidly activating delayed rectifier potassium channel. It exists between closed, open and inactivated states, with voltage dependent transitions between those states (Figure 2A). hERG exhibits unusual gating kinetics, with fast, voltage-dependent inactivation, and slow voltage-dependent deactivation. During an action potential, hERG is rapidly activated during the initial depolarization of the plasma membrane. However, very few potassium ions are conducted at this phase as the channel rapidly inactivates. As the action potential progresses, hERG slowly recovers from its inactivation, and conducts a large efflux of potassium ions during repolarization phase, which acts as the major mechanism bringing the transmembrane potential back to  $-85 \, \mathrm{mV}$ , and prevents the prolongation of the action potential duration (19,24).

#### 2.2 Isoforms of hERG.

In the cardiomyocyte, the hERG channel is a heteromeric tetramer consisting of two channel protein isoforms, hERG 1a and 1b (19,25,26). The two isoforms are products of alternative splicing, with identical mRNA sequences except for their 5' exons. hERG 1a mRNA translates into the "full length" form of the polypeptide containing 1,159 residues, whereas hERG 1b lacks the first 373 residues, replaced by a short and distinctive 36 residue N-terminus (19,25-27). 1a is the originally discovered and isolated isoform of hERG and is able to form highly functional homomers on the cell surface when expressed heterologously without hERG 1b. In contrast, homomers of hERG 1b subunits showed impaired maturation lacking detectable currents, but could be readily rescued by co-expression with 1a subunits (28-31). One possible explanation for the defective maturation of hERG 1b is the presence of an RXR endoplasmic reticulum (ER) retention signal found exclusively at the hERG 1b N-terminus, which is masked by the longer hERG 1a N-terminus when co-expressed (19,25,26).

As a result, much of our understanding of hERG is derived from heterologous expressions of hERG 1a alone (28,32-34). However, it is important to note that the current conducted by a hERG 1a homomer differs from that of a hERG 1a/1b heteromer. The native Ikr current kinetics are more closely mimicked by the heteromer, which exhibits more rapid activation and recovery from inactivation, resulting in a larger overall current magnitude, as well as an earlier peak during the action potential (Figure 2B). While it is certain that hERG 1a and 1b co-assemble in the cardiomyocyte, the stoichiometry and the assembly dynamics remain unclear. A recently proposed mechanism suggests that hERG 1a and 1b mRNA transcripts physically associate to facilitate heteromeric assembly. Another study showed evidence that the N-termini

from two subunits are sufficient to mediate heteromerization, suggesting the possibility that heteromerization can occur co-translationally (29,35).

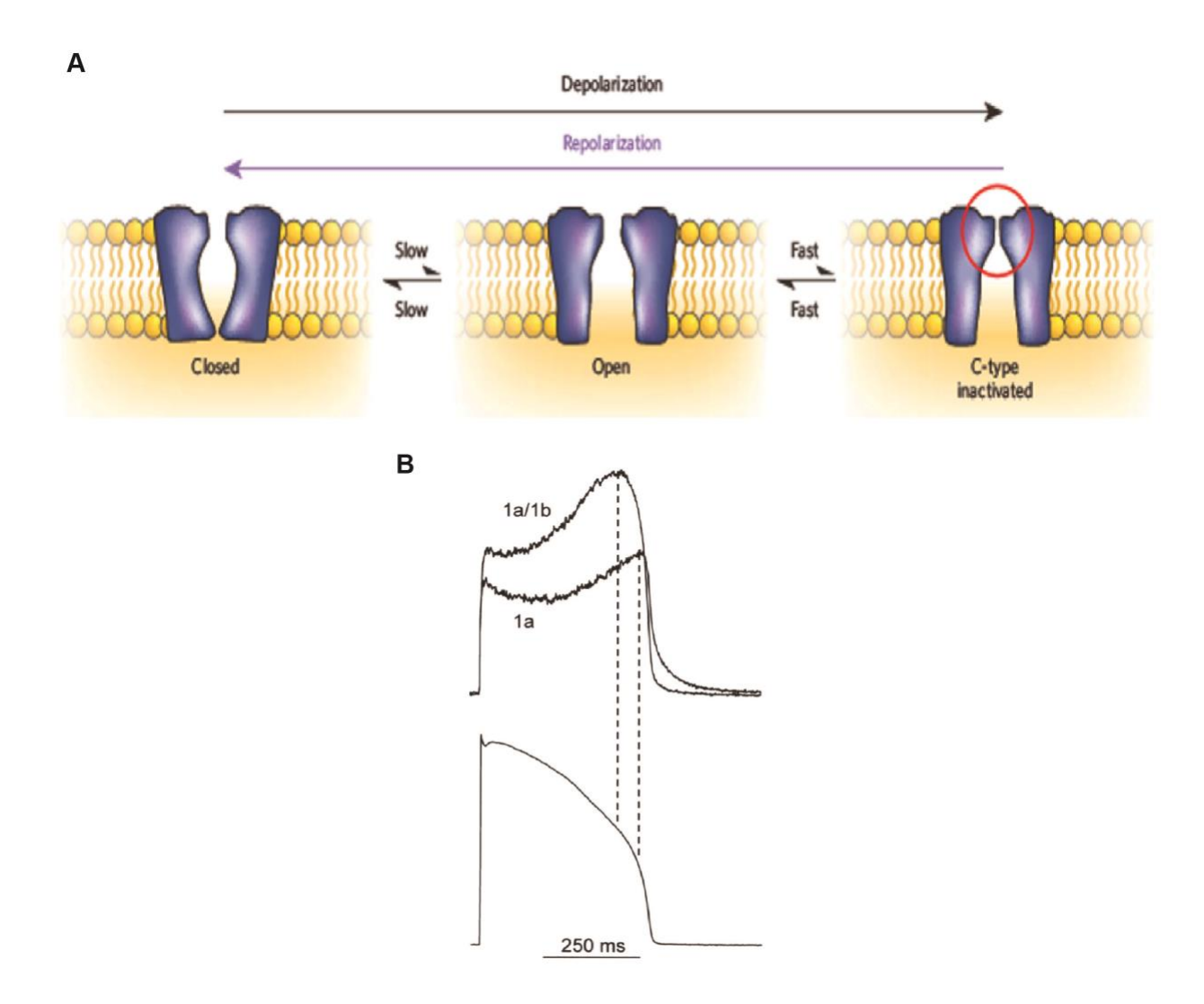


*Figure 2: Electrophysiological properties of hERG.* A: Schematic of hERG/I<sub>Kr</sub> channel in closed, open and inactivated states, as well as changes between states during depolarization and repolarization. Figure obtained from (36). B: hERG 1a homomer current, compared with hERG 1a-1b heteromeric current recorded during action potential clamp. Figure obtained from (32).

#### 2.3 Structural domains of hERG

The hERG 1a transcript gives rise to a 1,159 amino acid polypeptide chain, consisting of an N-terminal cytosolic Per-Arnt-Sim (PAS) domain, 6 transmembrane helices (S1-S6) and a C-terminal cytosolic cyclic nucleotide binding homology domain (CNBHD). The hERG 1b transcript encodes a shorter 819 residue polypeptide due to its divergent N-terminal sequence but is identical to hERG 1a from the transmembrane helices to the C-terminus. Unless otherwise stated, amino acid numbers are from the hERG 1a sequence.

#### *Transmembrane domains: the voltage sensor and the channel pore*

The S4 transmembrane domain acts as the voltage sensor of the channel. It contains 5 positively charged residues embedded in the membrane (K1, R2, R3, R4, R5), which act as gating charge transfer centers. When the membrane is depolarized, these residues are repelled towards the extracellular face, shifting the S4 helix upward and away from the channel pore axis (Figure 3A) (24). The S5 and S6 helices make up the ion conduction pore and the selectivity filter (19,24,37). Specifically, the ion conduction pathway is lined by the S6 helices from the 4 subunits; the S5 helices form the outer pore and is connected to S6 through a short semi-hydrophobic pore loop, containing the potassium ion selectivity sequence, Thr-Ser-Val-Gly-Phe-Gly (19,24,37). When a K+ ion passes through the selectivity filter, it is coordinated by the backbone carbonyl oxygen atoms of those residues (19,24,37). The recent cryo-EM structure of hERG (Figure 3B) reveals that during membrane depolarization, the shifting of S4 helix drives the opening of the channel pore in S5-S6, through direct mechanical coupling via a short S4-S5 linker. A glycine residue at the center of the S6 (G648) acts as a pivot point to enable widening of the channel base, allowing K+ ions to pass through (24,38). Additionally, the cryo-EM

structure provided insights into the unique central cavity of hERG, which contributes to its high susceptibility to be blocked by pharmacological agents. First, hERG features a small central cavity compared with other K+ channel, which makes the electronegative pore helices in closer proximity, resulting in an increasingly negative electrostatic potential that facilitates bindings to drugs containing positive charges. Additionally, there exist a small and elongated hydrophobic pocket extending from the central cavity of hERG into the pore helices (Figure 3B). This pocket is localized between the channel conduction pore and the selectivity filter and is absent in most other K+ channels. It is speculated that this hydrophobic pocket serves as a good binding site for functional groups of hERG blockers, further contributing to its high drug binding affinity.

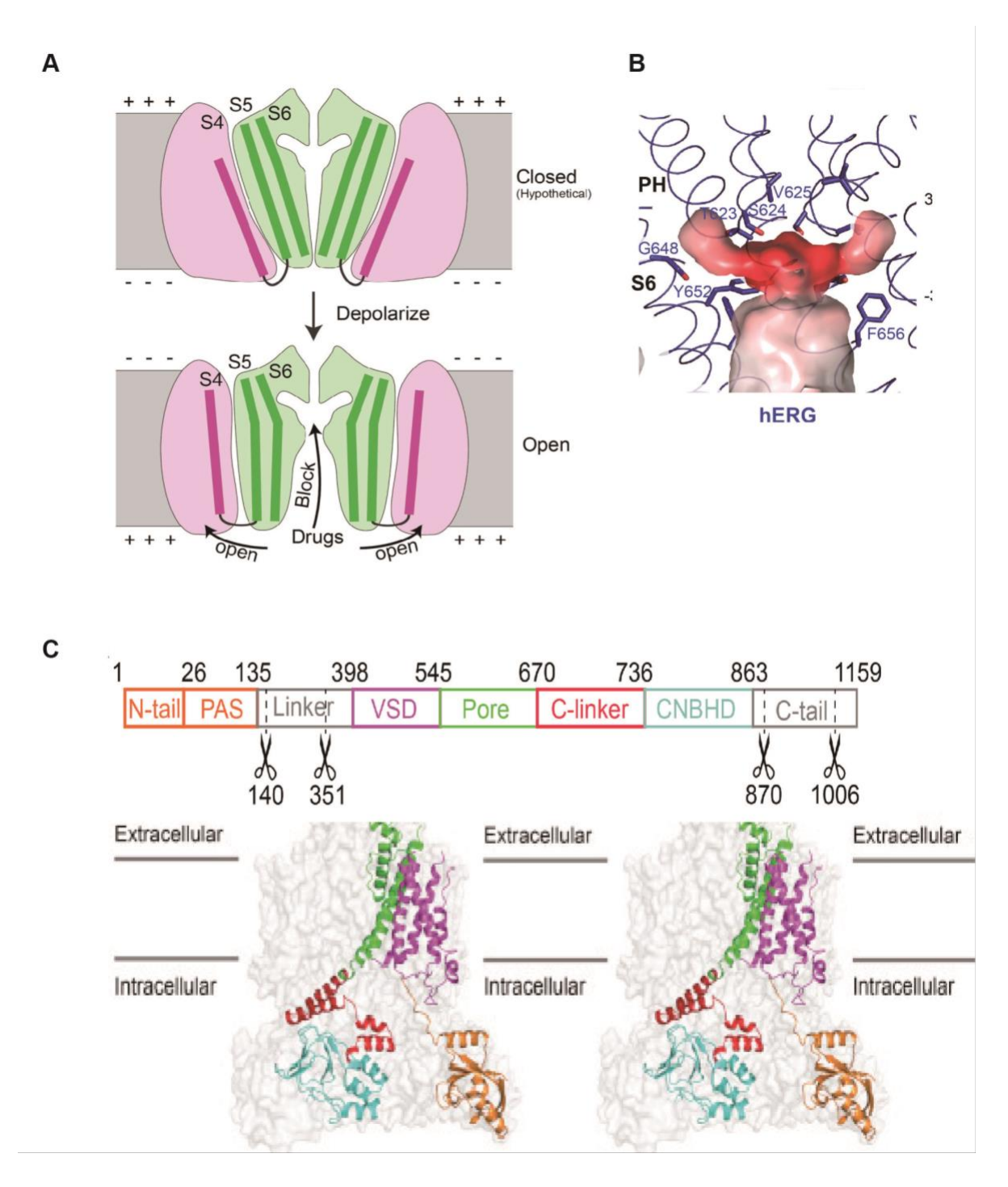


Figure 3: Cryo-EM structure of hERG. A: Graphical representation of hERG changing from close to open state. Conformational shift in the S4 voltage sensor is mechanically linked to the opening of channel pore. Figure obtained from (24). B: Space within the extended internal pocket in the hERG channel pore, colored in pink. Residues important to drug binding of hERG

are labeled with sticks, surrounding helices are shown in ribbons. Figure obtained from (24); C: Detailed domain structure of hERG subunit shown in the tetramer, embedded in the lipid Bilayer. hERG domains are color coded as map on the top. Note: in order to effectively purify hERG, areas in grey (linker of PAS-TM1, and distal C-terminus) were deleted from the sequence. Figure adapted from (24).

#### The cytosolic N-terminus and the PAS domain

The cytosolic N-terminus of hERG 1a contains a PAS domain (19,39), which is characteristic of the ether-a-go-go subfamily of K+ channels (19,40). The PAS domain, which is conserved in prokaryotic and eukaryotic species, generally functions in signal sensing and transduction (40,41). However, the PAS domain of hERG has been associated with the regulation of the channel's gating kinetics, particularly channel inactivation and deactivation. Mutations of the PAS domain, or of the N-terminus resulted in slowed inactivation and accelerated rate of recovery from inactivation, as well as an accelerated rate of deactivation (39,42-44). A crystallographic structure of the PAS domain reveals 5 central β-sheets as the core of the domain, surrounded by four  $\alpha$ -helices, with an important hydrophobic patch localized near the outer core. This hydrophobic patch has been shown to mediate interactions between the PAS and other hERG domains, especially the CNBHD (41,45-48). Although the mechanism by which PAS regulates deactivation remains unclear, its function seems to be dependent on its interaction with the C-terminus. Mutations of the hydrophobic patch, and mutations that disrupt its interactions with the CNBHD caused accelerated deactivation similar to N-terminus truncation mutants (48-51). In addition to the C-terminus, the PAS also interacts with the S4-S5 linker of the transmembrane domain, which may further contribute to gating (39,50). Since hERG 1b does not possess a PAS domain, it is thus not surprising that the hERG 1a/1b heteromeric channel display different channel gating kinetics than hERG 1a homomers (19,32).

## The cytosolic C-terminus and the CNBHD

The cytosolic C-terminus of hERG consists of C-linker and the CNBHD (19,29,52-54). The CNBHD does not bind any nucleotides but is instead occupied by a  $\beta$ -strand acting as an

intrinsic ligand (53,54). This ligand has been shown to be localized at the interface with the PAS domain, and participates in interdomain interactions, thus exerting an effect on channel gating (55). In addition, the C-terminal domain is important for the channel's maturation, trafficking and stability. Several studies showed that mutations of critical residues from this region often results in ER retention of the channel, and diminished cell surface expression (29,56-58). Studies have revealed the presence of an RXR ER retention signal within this region (residues 1005-1007), which causes ER retention of the channel when the sequence is exposed in C-terminal truncation mutants (31,59,60). The high resolution cryo-EM structure of hERG 1a tetramer showed that the C-linker and CNBHD from each subunit are arranged in a cytosolic ring below the transmembrane helices, with the PAS domains directly contacting CNBHDs from the neighboring subunit, at its outer surface away from the channel pore axis (24,38). Furthermore, through superimposing the open-state hERG cryo-EM structure with that of the close-state rEAG structure, it could be observed that the N-terminal PAS-cap loosely interacted with the C-linker and the end of S2-S3 domains in the channel's closed state. When the channel pore opened, this interaction was strengthened, entrapping the PAS-cap region in the C-linker helices, intracellular ends of the S2-S3 transmembrane loops as well as pre-S1 helices. This strengthened interaction can possibly contribute to stabilizing the open state of the channel (24,38). Lastly, the function of the C-terminus has also been linked to channel assembly/tetramerization, primarily from the discovery of a conserved tetramerization coiled coil domain (TCC) (19,24,61). However, the role of TCC, along with the C-terminus in hERG tetramerization has been a topic of debate, as multiple studies presented many contradictory findings (5,29,31,62,63).

#### 2.4 hERG synthesis, trafficking, and degradation

#### **Trafficking**

Like many secretory proteins, the synthesis and trafficking of hERG starts with transcription in the nucleus. There are three validated transcription start sites in the locus of KCNH2 gene that correspond to hERG 1a, 1b, as well as KCNH2-3.1, the channel isoform that is selectively expressed in neuronal tissues and will not be described in this thesis (19,64). The mRNA product is further processed in the nucleus before being exported to the cytoplasm for translation. During translation, the mRNA/ribosome/polypeptide complex is targeted to the ER leading to insertion of the first transmembrane helix into the ER membrane. In the ER, hERG polypeptides are folded and assembled into tetramers. The ER also serves as protein quality control site, whereby persistently misfolded polypeptides or complexes are directed towards the proteasome for degradation, so that only folded proteins or complexes are trafficked towards the cell surface. The processes of folding, assembly and degradation will be discussed in detail in the following sections. In the ER, hERG also undergoes N-linked glycosylation at N598 with a highmannose glycan (19,64). This form of hERG is considered as the immature, or core-glycosylated (CG). After hERG is folded and assembled into tetramers, it then exits the ER and is trafficked to the Golgi apparatus, where the N-linked glycosylation is modified to the final complex glycan (65). This modification increases the apparent molecular weight of the channel, and produces the mature, fully-glycosylated (FG) hERG. This glycosylation has been shown to stabilize hERG on the cell surface via decreasing its susceptibility to proteases (64,66). The perceivable size differences between CG and FG hERG also makes it convenient to estimate the trafficking efficiency of hERG with techniques such as SDS-PAGE. Upon leaving the Golgi apparatus, it is trafficked to the plasma membrane (PM). hERG has a calculated cell surface half-life of around 7 hours, and is then endocytosed from the plasma membrane, sorted in endosomal compartments, and eventually degraded in the lysosome (67). A general scheme of hERG trafficking is shown in figure 4A.

#### **Folding**

When a protein is properly folded, it adopts the conformation with the lowest free energy, where hydrophobic residues are buried in the interior, protected from exposure to the hydrophilic intracellular environment. The process of protein folding often requires assistance from molecular chaperones, which are specialized proteins that transiently bind to the exposed hydrophobic patches on the folding intermediates. This allows folding to proceed in a controlled manner and prevents aggregation of partially folded polypeptides. Additionally, molecular chaperones help to maintain a balance between protein folding and degradation. Should a polypeptide remain persistently unfolded due to a mutation or to environmental stress, it can be poly-ubiquitinated and targeted for degradation in the proteasome. In some cases, molecular chaperones assist in this degradation process. There are several pivotal chaperones which are involved in the processes of hERG folding and maturation, as well as its quality control in the ER.

Folding of hERG is dependent on the chaperone heat shock protein 70 kDa (Hsp70), its close homolog heat shock cognate 70 kDa (Hsc70), as well as heat shock protein 90 kDa (Hsp90) (19,27,68,69). Their role in hERG folding has been verified by multiple layers of evidence. Hsp/Hsc70 and Hsp90 have been detected in a proteomic interaction analysis conducted on hERG, and have been shown to physically interact with immature ER fraction of hERG via co-immunoprecipitations. Inhibition of Hsp90, as well as combined knockdown of Hsp70 and Hsc70 markedly impaired hERG maturation rate and surface expression (68-71). In addition, prolonged association was detected between hERG trafficking deficient mutants

R752W and G601S with Hsp70 and Hsp90, and this prolongation was reversed when the trafficking of G601S mutant was pharmacologically rescued (68,71). Hsp70 and Hsc70 are often interchangeable, with the major difference being that the expression of Hsp70 is typically stress induced, whereas Hsc70 is constitutively present. Despite the strong similarities between the two forms, they were suggested to exert opposing effects on hERG maturation, as overexpression of Hsc70 promoted hERG degradation and decreased hERG cell surface density, which was also achieved by knockdown of Hsp70 (68,72).

Hsp70 functions as a monomer, and in an ATP dependent manner. It cycles between an ADP-bound state with high affinity to its protein substrates, and an ATP-bound state of low affinity. Co-chaperones in the Hsp40 family such as DNAJA1 (DnaJ homolog subfamily A member 1, DJA1) are thought to recognize partially folded hERG polypeptides, mediate its transfer onto Hsp70, and stimulate ATP hydrolysis. Knockdown of DJA1 inhibited hERG maturation in HeLa cells (73). In addition, nucleotide exchange factors (NEF), such as BAG (Bcl2-associated athanogene 1) proteins, the Hsp110 family and HspBP1, are responsible for the release of substrate and ADP from Hsp70, and the subsequent re-binding of ATP (35,72). Hsp70 bound substrates can then be transferred to Hsp90 for further folding, via the Hsp-organizing protein (HOP) which interacts with both Hsp90 and the C-terminus of Hsp70, facilitating the substrate transfer. Of note, HOP shares the same C-terminal binding site as the E3 ubiquitin ligase CHIP (C-terminus of Hsp70 interacting protein), which has been shown to polyubiquitinate hERG for degradation (73).

Hsp90 also functions with an ATP dependent mechanism, as a homodimer. Briefly, it cycles between an open state and a closed state, with two intermediate states associated with large conformational changes between states (74). The open state is stabilized by HOP, which

mediates client protein transfer. ATP binding and hydrolysis triggers the transition from the open to the closed state (74). A small acidic protein, p23, stabilizes the closed state allowing the maturation of client protein. Upon the release of ADP, Hsp90 returns to its open state and releases its substrate. Several co-chaperones that are typically important for Hsp90 function can be found in detail elsewhere (74). They are not mentioned here, as their roles with hERG have not been determined. Binding of hERG by either Hsp90 or Hsc70-CHIP complexes seems to represent the bifurcation between maturation and degradation, as overexpression of Hsp90 resulted in increased levels of functional hERG proteins and hERG current, accompanied by decreased levels of CHIP binding (75).

#### Tetrameric assembly

The specific mechanism of hERG tetramerization, timing of the event, as well as the domains involved remain topics of debate. It is generally accepted that hERG subunit assembly is an ER event, from the observations that ER-retained mutants, as well as immature, coreglycosylated hERG 1b, were able to co-assemble with WT 1a subunits in co-immunoprecipitation experiments (29,60,76).

The identification of the tetramerization domain has been controversial. Deletion of a section of the C-terminus has been shown to impair tetramerization of rEAG channels, which share great structural similarities with hERG (77). A similar finding was also reported for hERG, and a C-terminal coiled coil domain, termed the tetramerization coiled coil (TCC, residues 1036-1074) was initially identified to be important for hERG subunit assembly (61). This was based on observations that: 1) Isolated hERG TCC fragments, in the presence of TCCs from other members of the EAG (*ether-a-go-go*) family rEAG-1and rEAG-2, were able to selectively form

hERG homo-tetramers in vitro; and chimeras of hERG with the TCC replaced with that from EAG-1 selectively tetramerized with EAG-1; 2) A frameshift mutation at the C-terminus eliminating this domain (residue 1035) caused impaired tetramerization of hERG detected by size exclusion columns, as well as diminished hERG currents (61). However, this study also found that the frameshift mutant was still able to be partially trafficked to the plasma membrane, and its loss-of-function phenotype could be partially rescued by disrupting an ER retention signal upstream of the mutation site. This contradicts the idea that the TCC is required for the tetramerization and function of the hERG channel. The involvement of TCC domain has also been challenged by other studies, as multiple other C-terminal truncation mutants showed normal trafficking and tetrameric assembly dynamics, including that of hERG 1a and 1b heterotetramers (5,29,30,62,63). All C-terminal mutants in the studies mentioned above are listed in Table 1. Of note, most of those mutants are not resolved in the hERG cryo-EM structure including that of TCC, as part of the C-terminus was removed during purification (24). However, one of the studies showed that hERG with deletion of residues 750-870 was able to form tetramers, demonstrated with sucrose sedimentation analysis (56). On the hERG cryo-EM structure, this segment makes up the main portion of the CNBHD, including a region that directly interfaces with the adjacent PAS domain. The lack of effect from this deletion, along with the data from other mutagenesis studies greatly challenges the role of C-terminal domains as the sole tetramerization domain.

Table 1: The effects of C-terminal mutations on hERG tetramerization, summarized from mutagenesis studies. SEC: size-exclusion columns; SGCA: sucrose gradient centrifugation analysis; WB: western blots; PC: whole cell patch clamp; Co-IP: co-immunoprecipitations.

Mutant	Mutant type	<b>Channel formed</b>	Experiment	Ref.
Q725X	Truncation	Monomer	SGCA	(58)
Δ750-870	Deletion	Tetramer	SGCA; WB	(56)
Δ860-899	Deletion	Tetramer	SGCA; WB	(57)
N861X	Truncation	Tetramer	Co-IP	(63)
G965X	Truncation	Tetramer	PC; Co-IP	(31,62)
R1014X	Truncation	Tetramer	PC; Co-IP	(31,62)
R1032X	Truncation	Tetramer	PC	(63)
Δ1034-1074	Deletion	Tetramer	PC; Co-IP	(62)
R1035X	Truncation	Monomer	SEC, PC	(61)
V1038X	Truncation	Tetramer	PC; Co-IP	(62)

Other regions of hERG have also been proposed to be related to tetramerization, as well as the possibility of multi-domain interactions, and the involvement of chaperones in the mechanisms of tetrameric assembly. One study found that both the cytosolic N-terminus including the PAS domain, and the C-terminus after the CNBHD are required for subunit recognition and assembly; double deletion mutants failed to tetramerize, and chimeras of the hERG with C- and N-terminal regions of EAG-1 showed selective heteromerization only with the EAG-1 channel (63). Another study reported in a liposome-supported cell free translation system, in vitro synthesized hERG was able to assemble into current-conducting tetramers, with the assistance from chaperones DNAJB12 and DNAJB14 (62). The binding of hERG to DNAJB12 and 14 was found to be at a 41 amino acid segment, spanning S6 and part of Cterminus (residues 639-679). Although DNAJB12 and 14 can interact with Hsp70 as cochaperones, Hsp70 was not required for this cell-free assembly (62). Studies of hERG 1a and 1b heteromerization also provided insights into the tetramerization process. In vitro co-expression of hERG 1a and 1b fragments containing only the N-terminus and the first two TM helices were shown to be sufficient to induce heteromerization (29). A similar effect was seen for isolated N terminal fragments of hERG 1a alone (78). In addition, a later study reported that mRNA transcripts encoding hERG 1a and 1b subunits can both be coimmunoprecipitated with antibody against the nascent hERG 1a protein. Moreover, shRNAs specifically targeting either hERG 1a or 1b transcripts reduced levels of both transcripts, when translation was inhibited (35). These findings suggest that the mRNAs of hERG subunits might be physically associated prior to translation to facilitate tetramerization, and that tetramerization might happen early in the folding process. However it has not been determined whether the assembly process is dependent on the N-terminus, due to insufficient mutagenesis data. The lack of unequivocal evidence for a single

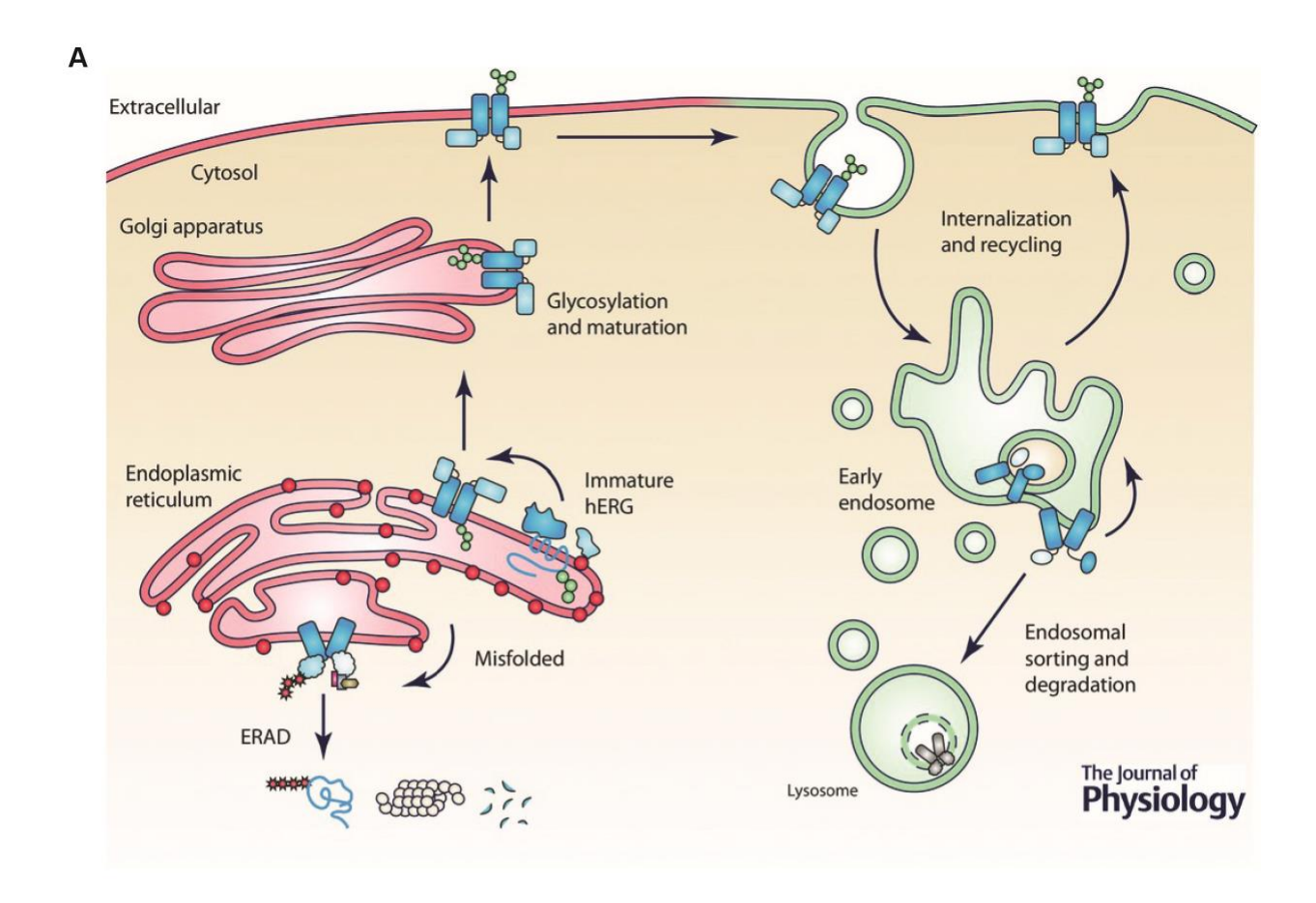
subunit assembly domain suggests the possibility of multiple domain involvement, or interdomain cooperation as the main mechanism of tetrameric assembly of hERG.

#### Quality control and degradation.

Quality control of hERG in the ER (ERQC) represents one of the most established mechanisms for LQT2 (57). Terminally misfolded mutants are degraded via ER-associated degradation (ERAD) system (Figure 4B). ERAD is comprised of an intricate network of proteins that perform serial steps leading to protein degradation, including substrate recognition, ubiquitination, transport into the cytosol and proteasomal degradation. As described previously, unfolded protein substrates were first associated with Hsp40 family proteins such as DJA1, DNAJA2 (DJA2) and DNAJA4 (DJA4), which mediate the substrate transfer onto Hsp/Hsc70 (57). At the C-terminus of Hsc70, CHIP attaches lysine 48-linked-polyubiquitin chains onto the incorrectly folded nascent hERG, which mark it for proteasomal degradation (73,79). CHIP is not the only E3 ubiquitin ligase that mediates hERG poly-ubiquitination. Rather, there seems to be a redundancy in E3 ligases that are involved this task. Recently, it was found that the ER resident E3 ubiquitin ligase TRC8 also mediates hERG poly-ubiquitination, with the help of Bag-1, a NEF of Hsp70, which induces release of hERG from Hsp70, and interferes with Hsc70-CHIP binding (70,80). Furthermore, E3 ligase RFFL (RING finger and FYVE-like domain E3 ubiquitin protein ligase) has also been linked to hERG polyubiquitination and degradation (70,80). After polyubiquitination, hERG is extracted from the ER membrane to the cytosol, where the proteasome is located. This retrotranslocation machinery has been suggested to involve the ATPase p97/VCP (80,81). p97 is a homohexomeric ATPase which extracts proteins substrate from immobile cellular structures such as membrane or multiprotein complexes, often

for proteasomal degradation (82). Overexpressing its dominant negative form caused defects in RFFL-mediating hERG degradation. Moreover, knockdowns of p97 adaptor proteins HERP and VIMP have been shown to stabilize the immature fraction of hERG mutant G601S (80,82). Lastly, the proteasome is a sophisticated cytosolic protease complex, consisting of a cylinder-shaped proteolytic core (20S proteasome) coupled with one or two regulatory particles (RP). The RP serves to recognize and translocate ubiquitinated protein to the 20s proteasome core, where they are subsequently cleaved by the catalytic threonine residues into oligopeptides of 3-15 residues (83).

In addition to ERAD, peripheral quality control systems are also engaged in hERG degradation. At the Golgi apparatus, hERG has been shown to be poly-ubiquitinated by the E3 ubiquitin ligase Nedd4, mediated by its interacting protein Ndfip1 (84). CHIP has also been shown to promote the removal of hERG from the plasma membrane, via K48- and K63-linked polyubiquitination (27,85). With ubiquitination as the sorting signal, tagged hERG channels were then rapidly endocytosed, sorted and trafficked through the endosome compartments to the lysosome, where they are degraded by proteolytic enzymes in the lumen (27,86). The role of cell surface quality control is especially evident in many PAS mutants, which exhibit mild ER retention but significantly decreased surface stability (27,67,85).



В

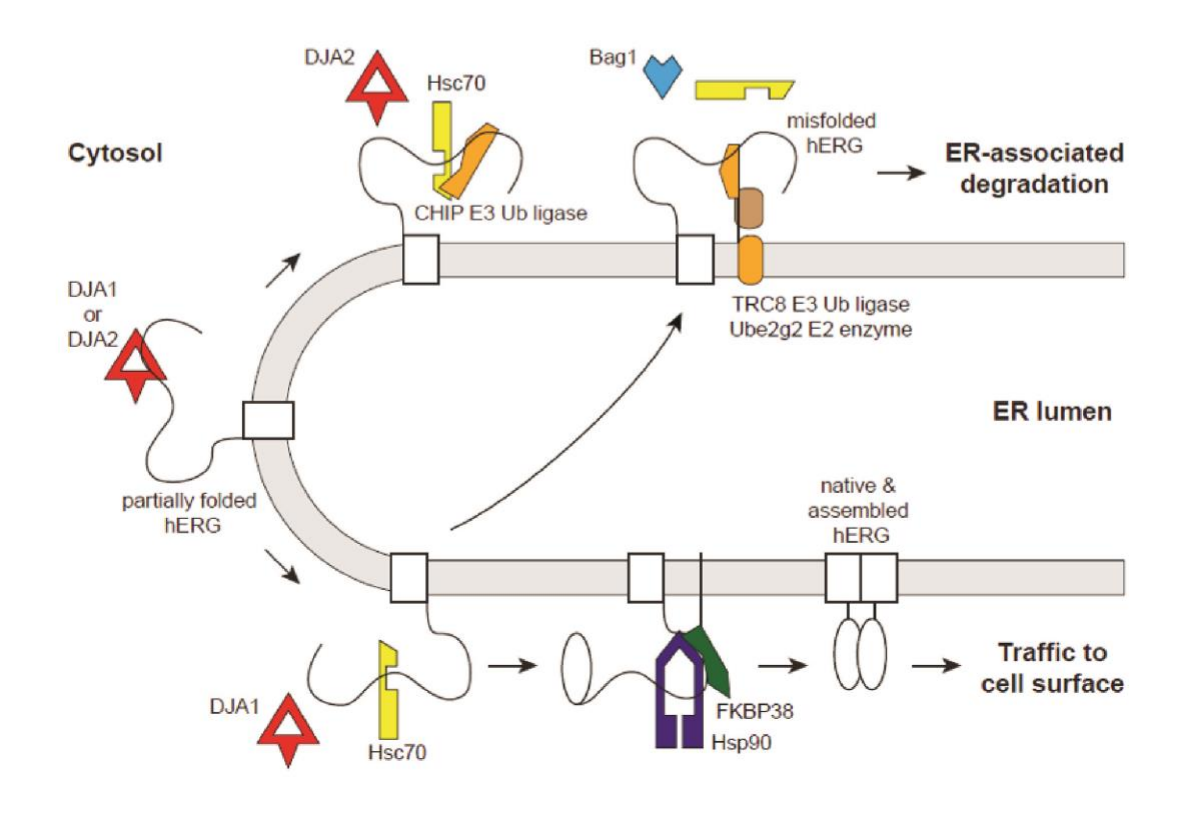


Figure 4: hERG trafficking and degradation pathways. A: Nascent hERG is first folded, assembled and glycosylated in the ER. Immature tetramer is then trafficked to the Golgi for further processing and complex glycosylation before reaching the cell surface. Channels can be endocytosed from the cell surface and sorted in the endosomes for lysosomal degradation. Figure obtained from (27). B: In the ER, nascent hERG subunits are loaded onto Hsp/Hsc 70 via DJA1/DJA2. It is then transferred onto Hsp90 via HOP, assisted by FKBP38. Alternatively, hERG is targeted by ERAD via E3 ligase CHIP, or by TRC8 via the assistance of NEF, Bag1. Figure created by J.C.Young.

#### 3. Mutations of hERG

#### 3.1 Types of hERG mutants

There are nearly 500 hERG mutations that have been linked to LQT2 (19,87). These mutants demonstrate a range of disease-causing molecular mechanisms, including abnormal synthesis, defective trafficking, impaired channel gating including reduced activation or enhanced deactivation, or altered ion permeability (19,87). Among them, trafficking defects are considered as the most common disease mechanism, accounting for about 88% of the all mutants studied (73,87-89). In many cases, the phenotype of the mutant can be correlated with the structural domain where it resides. Many mutations of the PAS domain can cause mild trafficking defects, but severe alterations in gating kinetics (84,87). In contrast, mutations of the channel pore region between S5-S6 as well as the CNBD domain can produce severe trafficking and maturation defects (52,87,90). Most of the trafficking mutants can be at least partially pharmacologically corrected with the hERG pore blocking drug E4031 and mutants of different domains differ in response to this agent (PAS domain, pore, and C-linker/CNBHD in order of effectiveness) (52,87,90). The mechanism underlying this correlation remains unclear, given the fact that only a small fraction of the LQT2 hERG mutants have been functionally characterized, so far.

# 3.2 Dominant negative vs Haploinsufficiency mechanism

Even though hERG mutant studies have relied on mutant 1a homomers as a model, in reality most LQT2 patients are heterozygous and inherit one mutant and one wild-type allele.

LQT2 is considered an autosomal dominant condition as the mutant takes dominance over the WT allele, and produces the disease phenotype. This mutant dominance effect can be explained

by the two classical genetic concepts, dominant negative and haploinsufficiency. Dominant negative (DN) refers to the scenario where the mutant allele impairs the function of the WT allele (91). In the case of a multimeric protein like hERG, it can be interpreted as the mutant allele co-assembling with that of the WT, causing degradation or abnormal functions of the entire complex (Figure 5) (91). Haploinsufficiency (HI) refers to the case where the mutant allele produces polypeptide that is degraded independently of WT but results in insufficient functional gene product. In multimeric protein complexes, mutant subunits may fail to interact or heteromerize with WT, and the disease is caused by a simple decrease in the number of functional subunits (Figure 5). To appropriately predict the consequences of LQT2 mutations on patients, subunit co-assembly dynamics should be taken into consideration since DN mutants would be expected to cause a more detrimental outcome than HI mutants. A recent mutant study of the LQT1-causing mutants of the channel KCNQ1 has shown that patients carrying DN mutations have significantly longer QTc interval and frequency of cardiac events than those carrying HI mutations (91,92). To my knowledge, no such study has been conducted on LQT2 mutants.

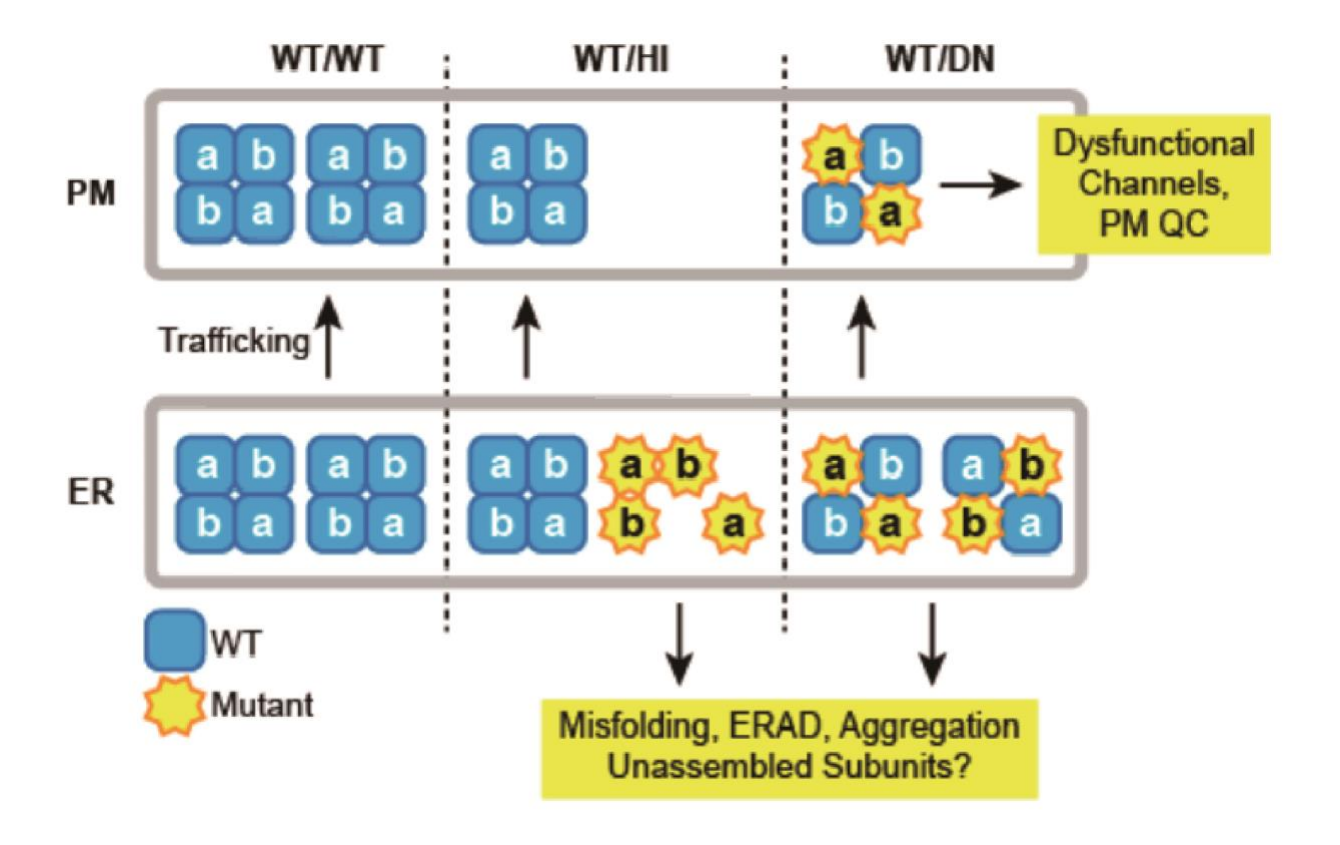


Figure 5: Proposed hERG trafficking scheme of WT channel, WT with dominant negative (DN) mutants, or with haploinsufficiency (HI) mutants. Left: WT 1a 1b heteromeric channels (blue) are assembled in the ER and trafficked to the plasma membrane. Middle: When WT hERG (blue) is expressed with that of HI mutant (yellow), HI mutants are degraded as either homotetramer or monomers, whereas WT homomeric channels are trafficked to the surface. Right: When WT subunits (blue) are co-expressed with DN mutants (yellow), the subunits hetero-tetramerize, causing degradation of the complex, or forming dysfunctional channels on the cell surface. Figure created by J.C.Young.

### 3.3 hERG mutants in the context of WT- mutant hetero-tetramerization.

Recent studies on hERG mutant-WT heteromers focused on either large-scale mutant screens, assessing the general pattern of traits from groups of mutants with a single technique (91,93), or single mutant studies where a few mutants are investigated in depth (70,76,93-97). The recent large-scale mutant analysis of 167 LQT2 mutants revealed that most mutations (76%) assessed in the pore region (S5-S6) as well as CNBHD exert a strict DN effect, visualized on immunoblot as the disappearance of FG bands when WT and mutants are co-expressed (88,91). In contrast, mutants of the PAS domain, S4-S5 linker and parts of the C-linker domain showed greater variability between mutants, and the phenotypes seem to be mutant-specific (91). However, mutations from those regions tend to have varied degrees of trafficking defects as homomers. Since the study did not use differentially tagged WT and mutant constructs, it is difficult to distinguish DN mutants with a moderate trafficking defects from severe HI mutant by simply detecting overall hERG signal on immunoblots. Recently, a high-throughput electrophysiology study of over 30 hERG mutants reported very similar results. All of the pore and CNBD mutant-WT heteromers assessed demonstrated >75% drop in the plasma membrane current (98). PAS domain and C-terminal tail mutants showed a range of current densities ranging from significantly reduced to similar as WT levels (98). Although these studies revealed a reproducible trend, more insight is required into the underlying mechanism.

DN and HI mutations have been analyzed by single mutant studies as well (96,97). Co-expression of the pore mutant G572S with WT hERG showed significantly diminished hERG current density, and poor plasma membrane expression. Co-immunoprecipitations (IP) and co-localization experiments demonstrated that the immature forms of WT and mutant subunits physically interact, and are both retained in the ER, consistent with a DN mechanism (97). In

contrast, a study characterizing G816V-WT heteromer showed that current density, as well as the level of fully glycosylated hERG expression is directly proportional to the level of hERG WT in the sample, suggesting an HI mechanism (96). Interestingly, despite following what seems like an HI mechanism functionally, significant physical interaction between the immature form of G816V and WT was still detected (70). It is possible that HI mutants can still associate with WT, but to a much lesser degree so that it does not significantly affect WT homomer formation. The findings of a list of single mutant studies are summarized in table 2.

Table 2: Summary of data from heteromeric hERG mutant studies. Mutant listed based on ascending amino acid number; mutants from high-throughput automated patch clamp study is listed separately. DN: dominant negative; HI: haploinsufficiency; Mild: mutant exhibit WT-like behavior; Indeterminant: heteromers was assessed but no conclusion could be drawn from the data presented; Co-IP: co-immunoprecipitation; PC: whole cell patch-clamp; SGCA: glucose gradient centrifugation analysis; WB: western blot.

Mutant	Type	Location	Phenotype	Experiments	Ref.
R25W (1B)	Miss-sense	N-terminal	DN	PC, WB	(99)
L65P	Miss-sense	PAS	DN	PC	(100)
L413P	Miss-sense	VSD	HI	PC	(101)
T421M	Miss-sense	VSD	Indeterminant	PC	(102)
D456Y	Miss-sense	VSD	HI	PC	(88)
F463L	Miss-sense	VSD	HI	PC, WB	(103)
N470D	Miss-sense	VSD	DN	WB, co-IP	(58)
T473P	Miss-sense	VSD	DN	PC	(104)
N474I	Miss-sense	VSD	DN	PC	(105)
G487R	Miss-sense	VSD	Mild	PC, WB	(106)
A558P	Miss-sense	Pore	DN	PC, WB	(107)
L559H	Miss-sense	Pore	HI	PC	(101)
A561V	Miss-sense	Pore	DN	PC	(108)
I571L	Miss-sense	Pore	HI	WB	(88)
G572S	Miss-sense	Pore	DN	WB, co-IP, PC	(97)
G584S	Miss-sense	Pore	DN	PC	(97)
I593R	Miss-sense	Pore	DN	PC	(109)
G601S	Miss-sense	Pore	HI	PC	(88,110)
G604S	Miss-sense	Pore	DN	PC, WB	(93)
A614V	Miss-sense	Pore	DN	PC	(105)
G628S	Miss-sense	Pore	DN	PC	(108,111)
V630L	Miss-sense	Pore	DN	PC	(105)
E637K	Miss-sense	Pore	DN	PC	(112)
Q725X	Truncation	CNBHD	HI	PC, co-IP, SGCA	(59)
R744P	Miss-sense	CNBHD	Mild	PC, WB	(94)
F805C	Miss-sense	CNBHD	HI	PC	(88)
G816V	Miss-sense	CNBHD	HI	PC, WB, co-IP	(96)
N861X	Truncation	CNBHD	DN	PC, co-IP	(63)
G965X	Truncation	C-tail	Mild- 1a/1a	PC, co-IP	(31)
			heteromer; DN- 1a-1b heteromer		

R1014X	Truncation	C-tail	Mild- 1a/1a	PC, co-IP	(31)			
			heteromer; DN-					
			1a-1b heteromer					
R1014X	Truncation	C-tail	DN	Co-IP, SGCA, PC	(59)			
P1085fx+32x	Frame shift	C-tail	Indeterminant	PC, co-IP, WB	(113)			
Mutant Data from High Throughput Heteromeric hERG Screen								
F29L	Miss-sense	PAS	DN	Automated PC	(98)			
N33T	Miss-sense	PAS	HI	Automated PC	(98)			
I42N	Miss-sense	PAS	DN	Automated PC	(98)			
R56Q	Miss-sense	PAS	Indeterminant	Automated PC	(98)			
L86R	Miss-sense	PAS	DN	Automated PC	(98)			
M124R	Miss-sense	PAS	Indeterminant	Automated PC	(98)			
A422T	Miss-sense	VSD	DN	Automated PC	(98)			
A561T	Miss-sense	Pore	DN	Automated PC	(98)			
A561V	Miss-sense	Pore	DN	Automated PC	(98)			
I571L	Miss-sense	Pore	DN	Automated PC	(98)			
G604S	Miss-sense	Pore	DN	Automated PC	(98)			
D609N	Miss-sense	Pore	DN	Automated PC	(98)			
T613M	Miss-sense	Pore	DN	Automated PC	(98)			
E614V	Miss-sense	Pore	DN	Automated PC	(98)			
L615F	Miss-sense	Pore	DN	Automated PC	(98)			
T618S	Miss-sense	Pore	Indeterminant	Automated PC	(98)			
N629I	Miss-sense	Pore	DN	Automated PC	(98)			
N629S	Miss-sense	Pore	DN	Automated PC	(98)			
N633S	Miss-sense	Pore	DN	Automated PC	(98)			
K638E	Miss-sense	Pore	DN	Automated PC	(98)			
R752W	Miss-sense	CNBHD	DN	Automated PC	(98)			
F805C	Miss-sense	CNBHD	DN	Automated PC	(98)			
S818L	Miss-sense	CNBHD	DN	Automated PC	(98)			
V822M	Miss-sense	CNBHD	DN	Automated PC	(98)			
R823W	Miss-sense	CNBHD	DN	Automated PC	(98)			
K897T	Miss-sense	C-tail	Indeterminant	Automated PC	(98)			
G903R	Miss-sense	C-tail	Indeterminant	Automated PC	(98)			
P1075L	Miss-sense	C-tail	Indeterminant	Automated PC	(98)			

# **Rationale and Objectives**

Large-scale hERG heteromeric mutant studies have found correlations between the domain location of a mutant and the likelihood of it being DN. Mutants of the pore/proximal CNBHD tend to follow a strict DN mechanism, whereas mutants of intracellular domains, such as PAS and distal CNHBD tend to show varied phenotypes. However, large scale studies have provided limited information regarding the underlying mechanisms that would explain the different trends. In depth studies characterizing heterozygous mutants are few, and among the studies conducted to date, there is a general lack of unified standards or approaches to identify, categorize and compare mutants. In addition, most heteromeric mutant studies did not separately tag WT hERG and mutant hERG thus, only indirectly observing the effect of mutant on the WT subunit.

Previous data from our lab, as well as other studies have found mutant specific responses in ERAD and the plasma membrane quality control processes, as well as distribution within the intracellular compartments. It is unclear how a DN mutant-WT heteromer would be recognized and processed in quality control systems, and if it would be differently handled from a WT or HI mutant homomer.

Thus, the objectives of the study are as follows:

- 1. To establish a systematic heteromeric expression system that allows observations of relative expression/behavior of WT and mutant subunits of hERG.
- 2. To survey a list of hERG trafficking mutants spanning different domains of hERG, and where possible differentiate DN from HI mechanisms.

# **Results**

### **Expression system and mutant selection**

Discriminating between DN and HI mechanisms requires examining WT subunit trafficking in the presence and absence of mutant subunits, as well as any physical association between WT and mutant subunits. Thus, WT and mutant constructs were tagged differentially for the study. A WT hERG 1a construct was made with a myc epitope tag inserted at the S1-S2 extracellular loop, while mutant (and WT) constructs were made with an HA epitope tag at the equivalent location. Tags inserted at this location were previously shown to not affect hERG trafficking or quality control (68).

First, the expression system was established. Transient expression of hERG in HeLa cells was compared to in HEK 293 cells, as both cell types were used in previous work by our laboratory (70,73). Transient expression allows precise control over expression levels and is convenient for assessing multiple mutant-WT combinations. On an immunoblot, the immature CG band of hERG 1a can be detected around 135 kDa, and the mature FG band can be detected around 155 kDa (Figure 6A). HeLa cells lack endogenous hERG expression, and are able to show the hERG FG band that is distinguishable from the CG band, while the FG band is often smeared in HEK 293 cells (Figure 6A), thus HeLa cells were used for all downstream experiments. Next, to ensure that plasmid quantity used in transient transfections does not exceed the protein production capacity of the cells, an increasing dosage of 1-4 µg WT<sub>myc</sub> plasmids were tested. A corresponding linear increase in hERG signal was observed on myc immunoblots, and 2 µg hERG plasmid appears to be within the proper limit (Figure 6B). Thus 2µg of total ion channel plasmids (1 µg mutant + 1 µg WT) was chosen for heteromer experiments.

Transient transfections tend to produce high level of proteins in the cells. To verify that the amount of polypeptide produced does not overwhelm the ER folding machinery, the

Unfolded Protein Response (UPR) was also tested. As name suggests, the UPR is an ER stress response, which counters the accumulation of unfolded proteins in the ER lumen by upregulating the ER folding and degradation machinery, downregulating translation and inducing apoptosis (51). In this case, the level of BiP (Binding Immunoglobin Protein), the ER resident form of Hsp70 was assessed. Upregulation of BiP was observed with administration of the agent Thapsigargin, a known UPR inducer (Figure 6C). The expression of BiP was low in the untransfected DMSO control, and similar with co-transfections of WTmyc with either WThA or severe trafficking mutants G601ShA and F805ChA, suggesting that ER stress has not been triggered by 2 µg plasmid transfections of WT hERG with mutants. These experiments suggest that effects of WT and mutant hERG polypeptides on each other are unlikely to be caused by transfection artefacts related to the ER quality control system.

An extensive list of LQT2 associated hERG trafficking mutant candidates was selected to be analyzed for this study (Figure 7A). The mutant selection criteria were as follows: 1) Mutants were originally identified in LQT2 patients, documented in the Inherited Arrythmia Database (http://triad.fsm.it/cardmoc/). 2) Based on the cryo-EM structure of hERG, mutants were expected to disrupt each domain and domain interface, focusing on mutation hotspots such as the pore and the C-linker/CNBHD region. 3) Priority was given to severe trafficking or gating mutants for ease of comparison. Uncharacterized mutants were also chosen, especially those with non-conservative amino acid substitution. Among the extensive list of mutants, 5 were selected for this initial study: G306W, A561V, G601S, F805C, G816V. These included two severe trafficking mutants that we had previous experience working with (G601S, F805C), two mutants with existing information in the literature regarding possibilities of being DN or HI (A561V, G816V), and an uncharacterized mutant with a drastic amino acid substitution (G306W) (96,97).

On the hERG structure, G306W is in the N-linker between the PAS domain and the S1 transmembrane domain, A561V and G601S are in the pore region, and F805C and G816V are in the CNBHD (Figure 7B). These mutants serve as the starting point of a potential systematic mutant survey.

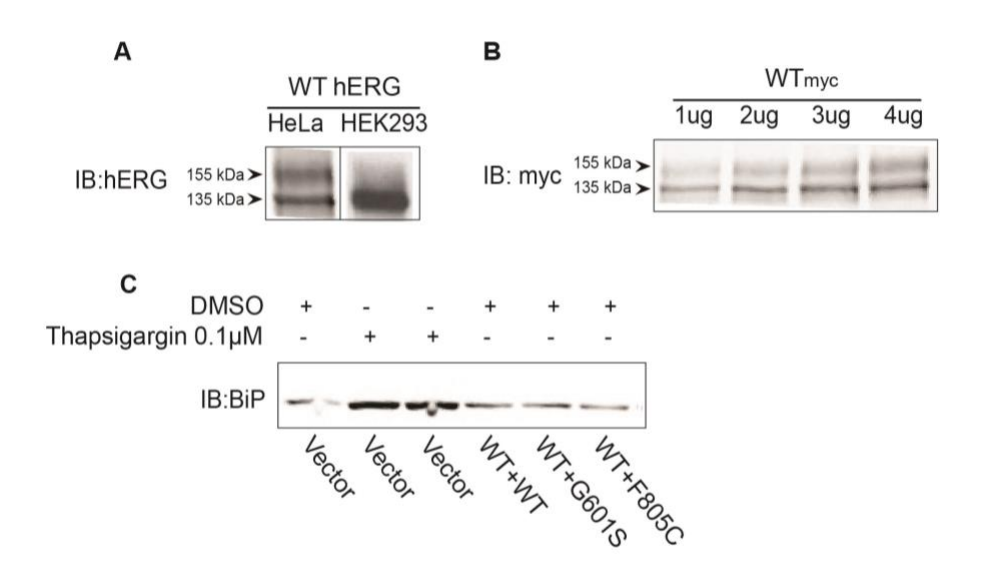
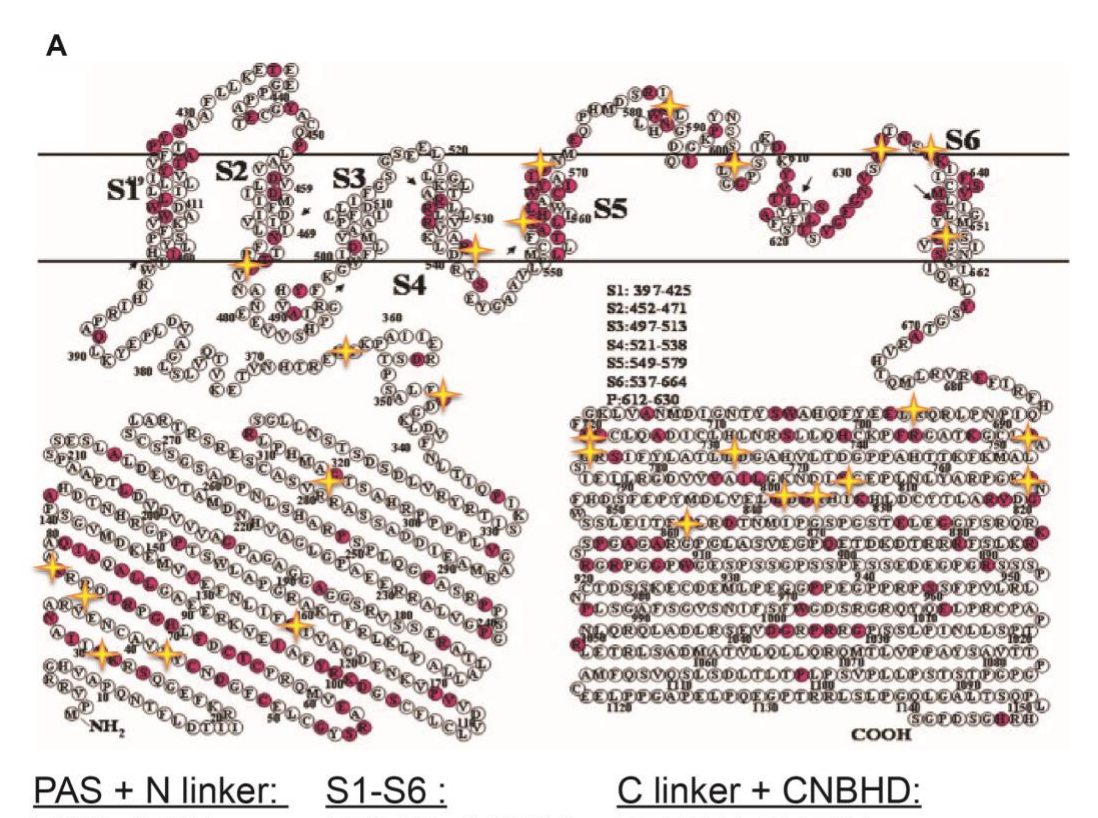


Figure 6: Expression system and Unfolded Protein Response. A: Immunoblots showing transient transfections of 2 μg hERG plasmid in HeLa (left) or HEK 293 (right) cells, detected with anti-hERG antibody. B: Increasing dosage of 1-4 μg hERG WTmyc plasmids transfected in HeLa cells, detected with anti-myc antibody. C: HeLa cells were transiently transfected with 2 μg total plasmids, consists of equal amount of either WTmyc+WThA, WTmyc+ G601ShA, WTmyc+F805ChA, or 2 μg of vector alone, and incubated for 24 hours with either DMSO or 0.1 μM Thapsigargin at 24 hours post transfection. The Unfolded Protein Response was assessed by immunoblots detected with anti-BiP antibody.



PAS + N linker: F29L, I42N, T65P, 192L, M124R, G306W, G601S, P632S, G816V, S818P, P347S

S1-S6: R534C, A561V, G572S, G584S, G785V, F805C, E637D, F656C

C linker + CNBHD: R752W, D774Y, R835W, D837G, N861H,

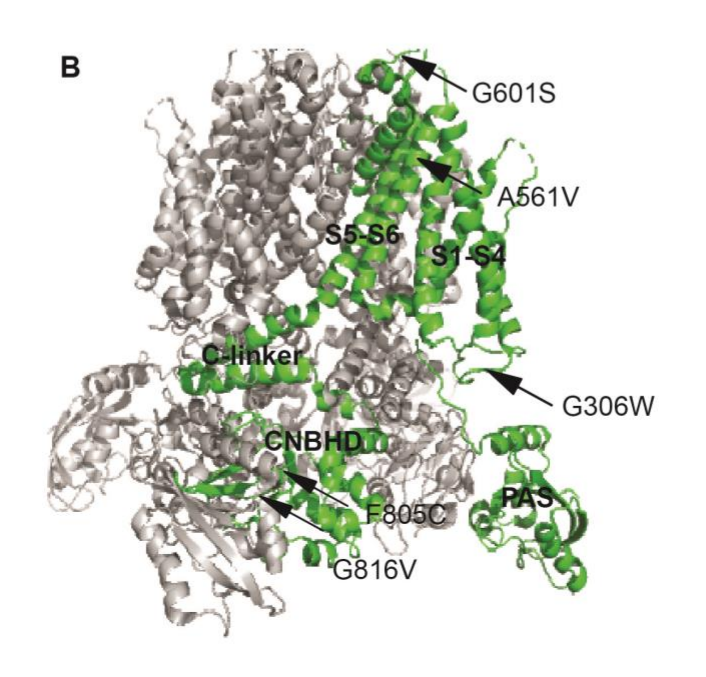
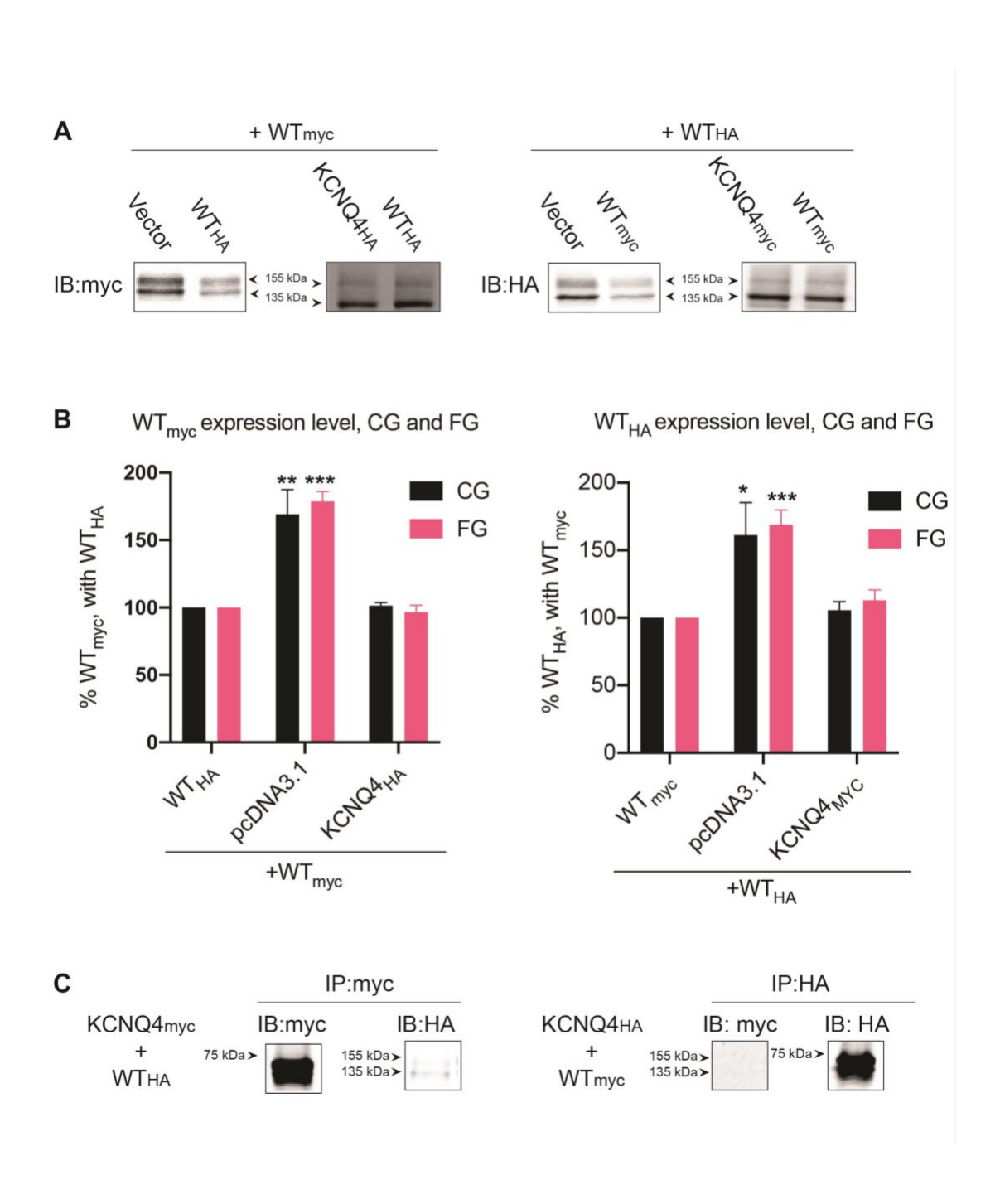


Figure 7. Selection of hERG mutants. A: Schematic (top) and list (bottom) of mutants selected for the study, sorted by domain location. Mutation locations are marked on the schematic with golden stars. All mutants are LQT2-associated, chosen from the Inherited Arrhythmia Database. Schematic modified from (114). B: Tetrameric hERG structure, with one subunit highlighted in green. The location of the 5 mutations selected for this study is indicated on the green subunit with arrows. The location of each domain is labeled in bold. Figure based on (24).

#### Effects of hERG mutants on maturation of hERG WT

To assess if mutant hERG subunits disrupt WT function, each HA-tagged mutant was co-expressed with myc-tagged WT in HeLa cells. The effects of WT on the trafficking defects of the mutants could also be observed. As controls, WT<sub>myc</sub> (or WT/mutantha) was co-expressed with WTHA (or WTmyc), or an equal amount of control ion channel KCNQ4HA (or KCNQ4myc), respectively. KCNQ4 acts as a "space-filler", its significance is two-fold: first, to keep the overall plasmid quantity consistent across samples, and second, to measure WT (or mutant) hERG expression and maturation without the effect of mutant (or WT), mimicking the scenario of 1 µg hERG WT or mutant expressed alone. Conceptually, KCNQ4 represents a null hERG allele. It was used instead of the conventional empty vector control, due to the observation that when vector was used, 1 µg of WTHA (and WTmyc) plasmid consistently produced more protein product compared to when co-expressed with WT<sub>myc</sub> (or WT<sub>HA</sub>) (Figure 8A). A possible explanation of the enhanced hERG expression is the absence of protein product produced by vector. The lack of protein product renders the ER, the secretory pathway as well as the plasma membrane more available to the polypeptides produced from the hERG plasmid, thus indirectly aiding its processing and expression. The use of control ion channel KCNQ4 successfully reversed this artefact and similar amounts of WTHA was observed, when expressed with WTmyc or with KCNQ4<sub>myc</sub> (Figure 8A). Similar changes were also observed with WT<sub>myc</sub> expressed with empty vector or KCNQ4HA (Figure 8A and B). KCNQ4 was chosen as control over a number of ion channel plasmids tested because it produced bands on immunoblots that overlapped the least with those of hERG, and displayed the least cross-antibody reaction (data not shown). There has been no significant evidence in the literature which suggests KCNQ4 might interfere or boost hERG trafficking. Similarly, no significant effect was found on hERG expression and

maturation, and no physical interaction by co-immunoprecipitation has been detected in this study (Figure 8C).



*Figure 8. Selection of KCNQ4 as control plasmid.* HeLa cells were transiently transfected with myc or HA tagged WT+ WT, WT+ pcDNA3.1 or WT+ KCNQ4. Relative expression of WT<sub>myc</sub> and WT<sub>HA</sub> in each case was detected with anti-myc or anti-HA antibodies. A: Sample myc (left) and HA (right) immunoblots showing WT<sub>myc</sub> (or WT<sub>HA</sub>) relative expressions. B: Quantifications of WT<sub>myc</sub> (left) and WT<sub>HA</sub> (right) CG and FG signal intensities. Values normalized to signals of WT-WT, to enable comparison between pcDNA 3.1, and KCNQ4. For anti-HA immunoblot: WT n= 4; pcDNA 3.1 n= 5; KCNQ4 n= 3. For anti-myc immunoblot: n= 4 for WT, pcDNA3.1 and KCNQ4. Error bars denote SEM. \*, p ≤ 0.05; \*\*, p ≤ 0.01; \*\*\*, p ≤ 0.001 (All data n ≥ 3). C: HeLa cells transiently transfected with KCNQ4<sub>myc</sub> with WT<sub>HA</sub>, or KCNQ4<sub>HA</sub> with WT<sub>myc</sub>, and were immunoprecipitated with anti-myc, anti-HA magnetic beads respectively. Samples were then immunoblotted with anti-myc, or anti-HA antibody, to detect possible associations between hERG and KCNQ4 plasmids.

After co-expression with mutantha, the resulting WT<sub>myc</sub> levels were assessed by myc immunoblots, compared with control sample (WT<sub>myc</sub>+WTha). No significant changes in the WT CG form was observed for any of those 5 mutants (Figure 9A-B). However, a significant decrease in FG form of WT was observed with pore mutants A561V and G601S, but not with C-terminal mutants F805C and G816V, or the N-linker mutant G306W (Figure 9B). The results suggest impaired WT subunit maturation by co-expression with A561V and G601S, and is consistent with a DN mechanism. On the other hand, the lack of an effect for the C-terminal and N-linker mutants suggests WT maturation and processing are not affected by these mutants, thus following an HI mechanism. However, it should be noted that the G306W homomer traffics well (Figure 10A), thus the result can be explained by the benign WT-like trafficking phenotype of the mutant.

Mutant levels were assessed via HA immunoblots comparing signals of mutantha (or WTha), in the presence of either WTmyc, or KCNQ4myc. Grossly, there were no significant effect of WT found on both the CG and FG levels of most of the mutants (Figure 10A-C). The only exception was that the FG of G601S was significantly increased by co-expression with WT subunit, resulting in a faint FG band on the blot, which was otherwise absent (Figure 10A and 10C). This result demonstrates that WT subunits potentially promote maturation of the G601S mutant, but not the other mutants assessed, suggesting the possibility that WT and G601S form a heterotetramer, in the context of a DN mechanism.

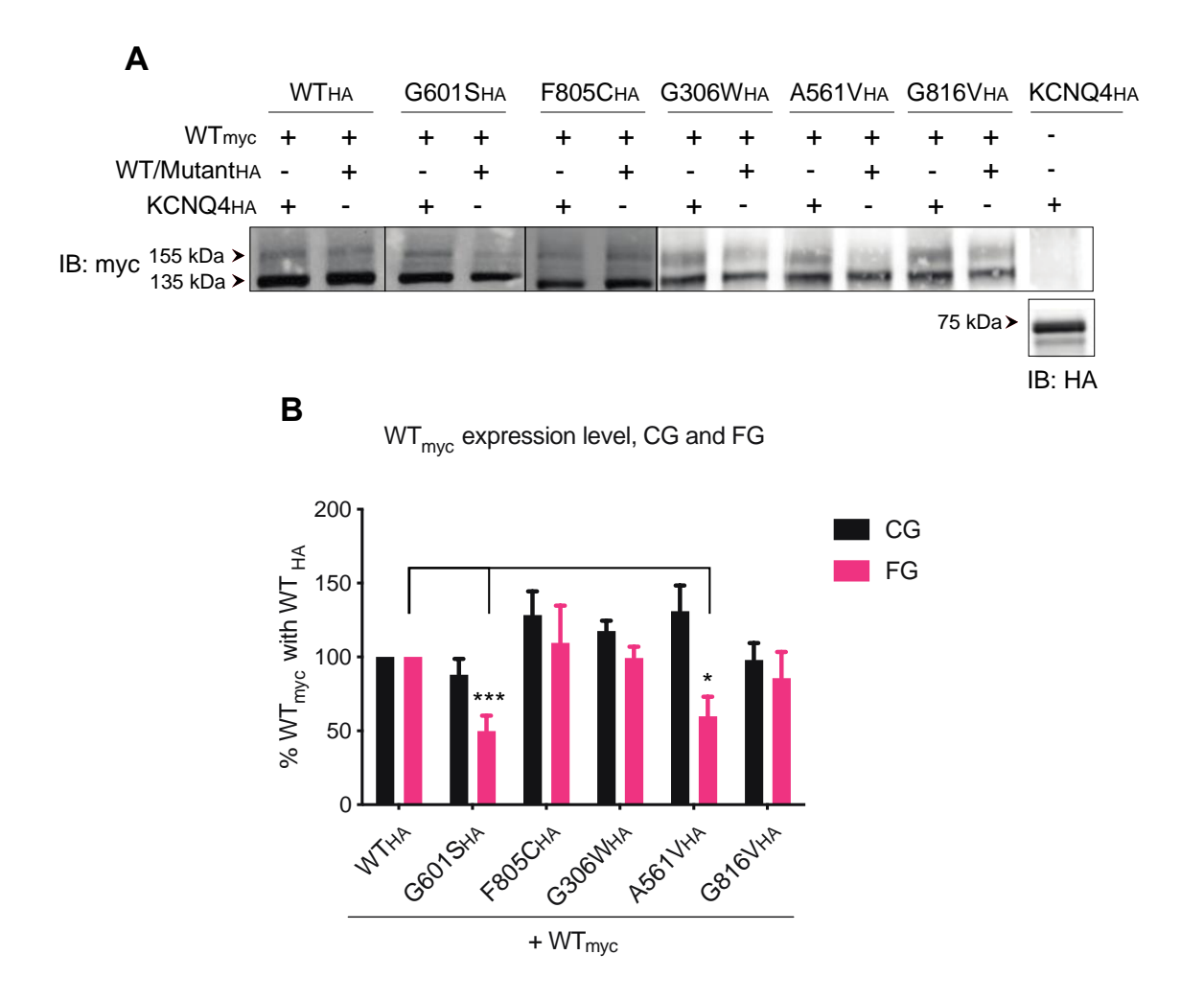
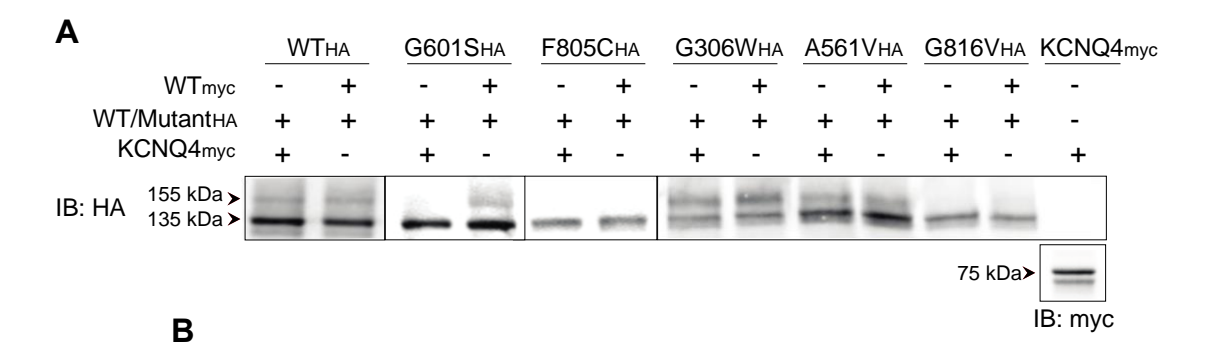
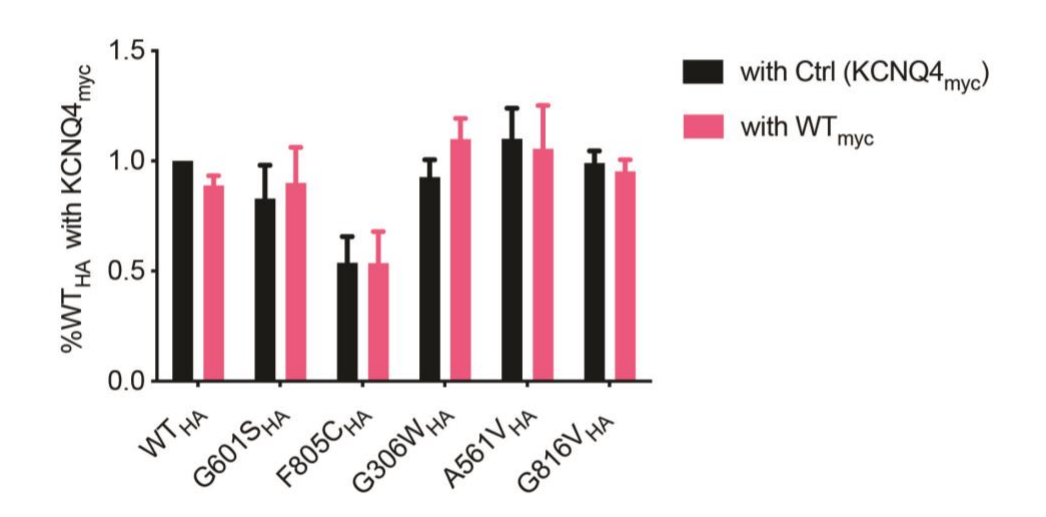


Figure 9: Effects of hERG mutant on WT subunits. A: Sample immunoblots showing HeLa cells transiently transfected with either WT<sub>myc</sub>+WT<sub>HA</sub> or mutantha hERG, or WT<sub>myc</sub>+control channel KCNQ4ha. Relative expression of WT<sub>myc</sub> was assessed with anti-myc antibody. B: Quantifications of CG and FG WT<sub>myc</sub> intensities detected by anti-myc immunoblot at 135 kDa and 155 kDa, respectively. Values were normalized to WT<sub>myc</sub> expressed with WThA to enable comparisons. WT and G816V n= 4; G601S, A561V and F805C n= 5; G306W n= 3. Error bars denote +/- SEM. \*, p  $\leq$  0.05; \*\*, p  $\leq$ 0.01; \*\*\*, p  $\leq$ 0.001.



Mutant<sub>HA</sub> (and WT<sub>HA</sub>) expression level, CG



 ${\bf C}$   ${\bf Mutant_{HA}~(and~WT_{HA})~expression~level,~FG}$ 

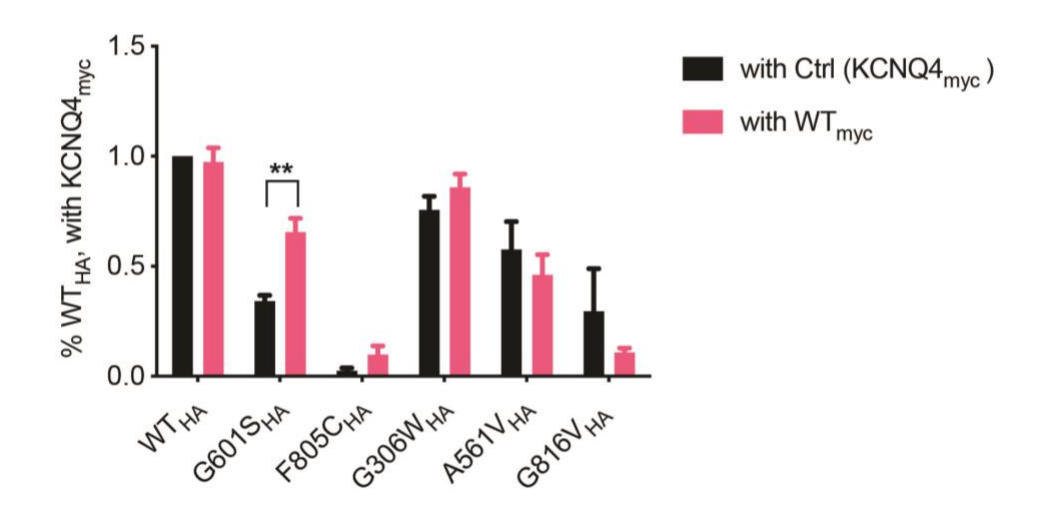


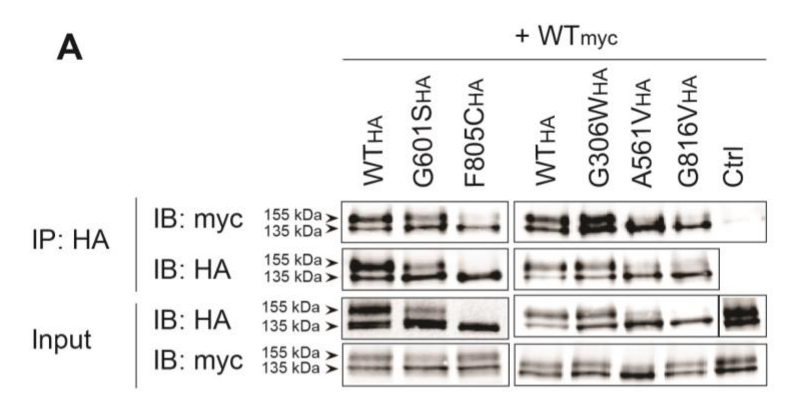
Figure 10: Effects of hERG WT on mutant subunits. A: Sample immunoblots showing HeLa cells transiently transfected with either mutantha (or WThA) +WTmyc, or mutantha (or WThA) + control channel KCNQ4myc. Relative expression of mutant was assessed with anti-HA immunoblots. B-C: Quantification of CG (B) and FG (C) mutant signal intensities were detected by anti-HA antibody at 135 kDa and 155 kDa, respectively. Values were normalized to WThA expressed with KCNQ4myc to enable comparisons. WT n= 4; G601S, F805C and G816V n= 5; G306W and A561V n= 6. Error bars denote +/- SEM. \*,  $p \le 0.05$ ; \*\*\*,  $p \le 0.01$ ; \*\*\*\*,  $p \le 0.001$ .

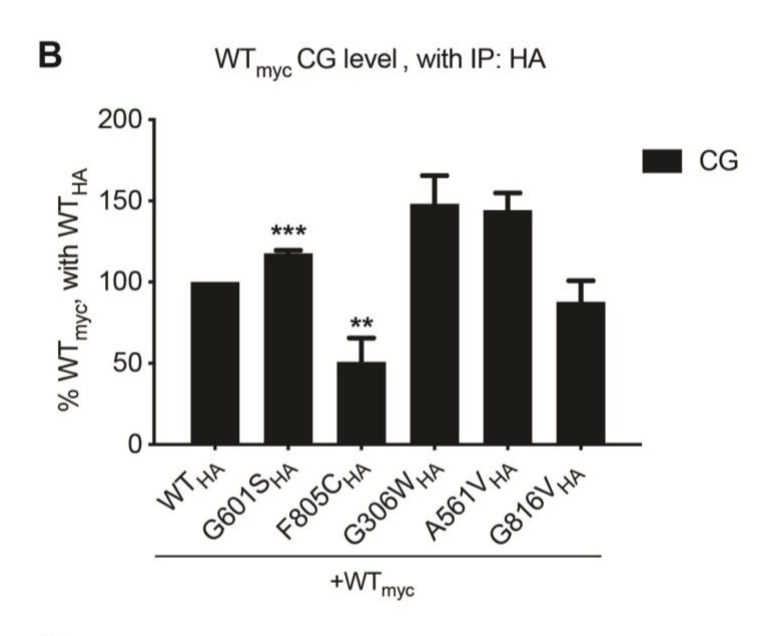
### Interaction of mutant and WT subunits

To investigate whether WT and mutant subunit physically interact with each other, whole cell lysates from the co-expression experiments were immunoprecipitated with anti-HA antibody for mutants, and subsequently detected with anti-myc antibodies for WT hERG (Figure 11). The reverse experiment was also performed (Figure 12). As controls, WT<sub>myc</sub> clearly interacted with WTHA (Figure 11A and 12A), and negative controls of WTmyc lysates mixed with that of WTHA post-harvest showed no interactions (Figure 11A and 12A). For the N-linker mutant G306W, WT and mutant were both pulled down by each other at levels either equivalent, or even higher than that of WT<sub>myc</sub>+WT<sub>HA</sub>, suggesting extensive interactions between WT and G306W subunits (Figure 11-12). For A561V and G601S mutants, significantly higher levels of WT<sub>myc</sub> CG were found associated with mutants, compared to WTHA (Figure 11B). The reverse was also true, though only qualitatively observed (Figure 12B). FG interactions were both low, but were detectable on immunoblots (Figure 11A). However, since the expression of WT FG was significantly reduced as a result of co-expression with the two mutants (Figure 11, Total IB: myc), the extent of interactions between WT and the two pore mutants could be underrepresented by the co-IP result compared with other mutants by which WT levels were not affected. For C-terminal mutants F805C and G816V, there were either significantly (F805C) or qualitatively (G816V) less CG interactions between WT and mutants (Figure 11A-B), and minimal, and almost non-detectable FG interactions (Figure 11A, 11C, 12A, 12C).

Overall, these results suggest that 1) all mutants physically interacted with WT subunits in the CG form. 2) The N-linker mutant G306W showed interactions similar to WT-WT. 3) The two pore mutants showed extensive CG interactions with WT, but reduced FG interactions, and 4) The two CNBHD mutants showed both decreased CG and minimal FG interactions with WT.

Thus, none of the mutants appeared to have a "pure" HI mechanism, in which mutant subunits never interact with WT. However, partial HI effects may be possible for F805C and G816V, as co-expression with these two mutants had no effect on the expressions of WT subunit on the immunoblots.





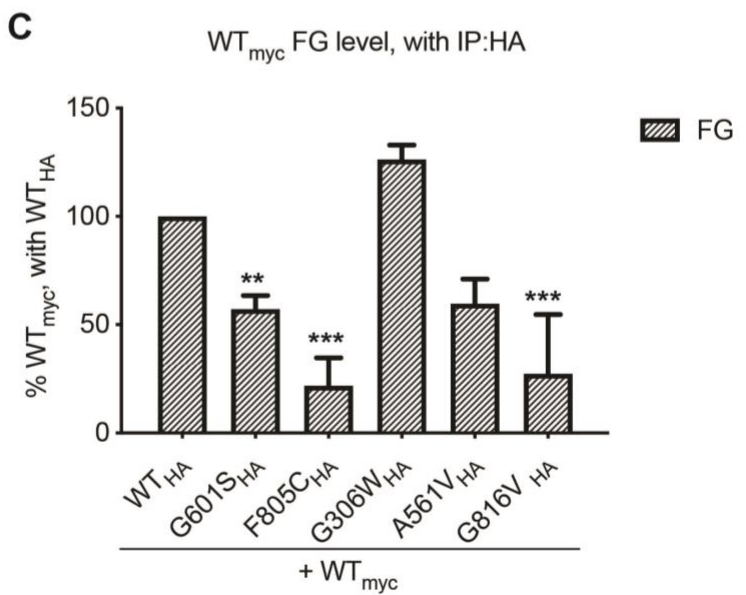
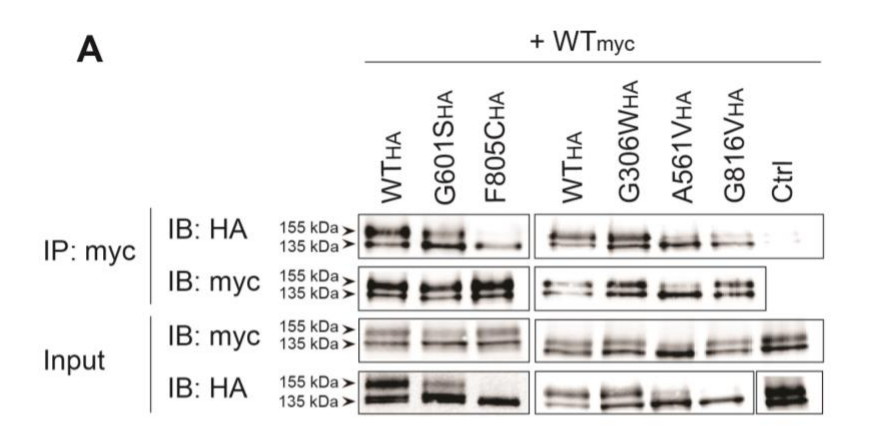
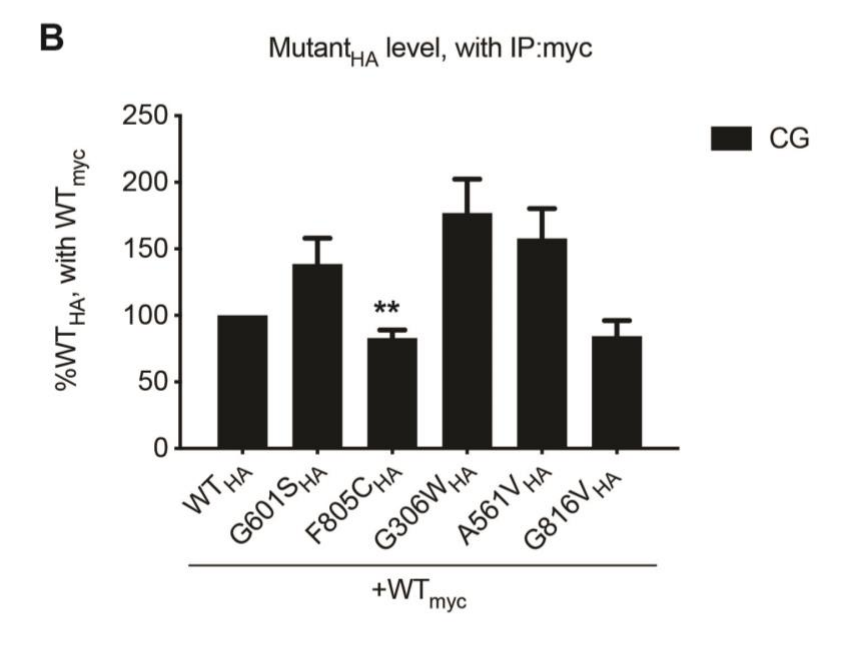


Figure 11: Interaction of hERG WT with hERG mutants. HeLa cells were transiently transfected with mutantha (or WTha) +WTmyc hERG. Lysates were immunoprecipitated with anti-HA magnetic beads, signals were detected with anti-HA and anti-myc antibodies to assess levels of WTmyc co-immunoprecipitated with each mutant. A: Immunoblots (IB) showing mutantha (or WTha) and WTmyc levels in samples immunoprecipitated with anti-HA antibody (IP:HA), or originally in the samples (Total). The negative control (rightmost lane) was WTmyc lysate mixed with WTha post-harvest, and immunoprecipitated with anti-HA antibody. B-C: quantification of CG (B) and FG (C) WTmyc signal intensities, normalized to WTmyc co-immunoprecipitated with WTha to enable comparison between mutants. WT, G601S, F805C, A561V and G816V n= 3; G306W n= 2. Error bars denote SEM. \*, p \le 0.05; \*\*, p \le 0.01; \*\*\*, p \le 0.001.





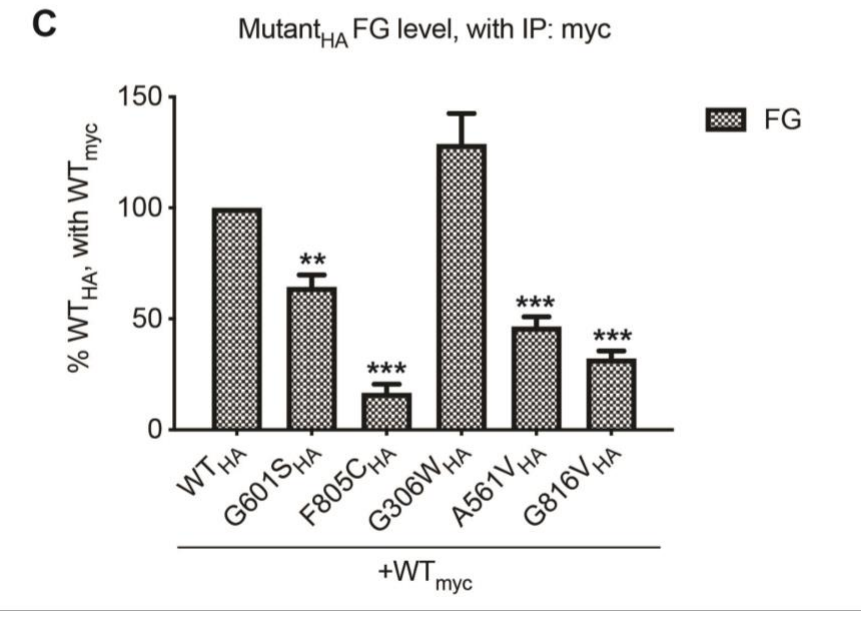


Figure 12: Interaction of hERG mutants with hERG WT. HeLa cells were transiently transfected with mutantha (or WTha) +WTmyc hERG. Lysates were immunoprecipitated with anti-myc magnetic beads, signals were detected with anti-HA and anti-myc antibodies to assess levels of mutantha co-immunoprecipitated with WT. A: Immunoblots (IB) showing mutantha (or WTha) and WTmyc levels in samples immunoprecipitated with anti-myc antibody (IP: myc), or originally in the samples (Total). The negative control (rightmost lane) was WTmyc lysate mixed with WTha post-harvest, and immunoprecipitated with anti-myc antibody. B-C: quantification of CG (B) and FG (C) mutantha signal intensities, normalized to WTha co-immunoprecipitated with WTmyc to enable comparison. A561V, G601S and G816V n= 3; G306W n= 2; F805C n= 4. Error bars denote SEM. \*, p  $\leq$  0.05; \*\*, p  $\leq$  0.01; \*\*\*, p  $\leq$  0.001

#### **Discussion**

The functional defects in the majority of LQT2 mutants have been attributed to aberrant hERG trafficking, resulting in a loss of potassium current on the cell surface and thus impaired ventricular repolarization in cardiomyocytes. A mechanistic understanding of hERG trafficking mutants would contribute towards finding ways to restore hERG cell surface density, thus providing therapeutic potential. In addition, the heterozygous nature of hERG in LQT2 patients stresses the importance of examining mutant behavior in the context of mutant-WT heteromers, and exploring mutant-WT subunit interaction dynamics as a relevant mutant mechanism. This study examined the effect of five hERG trafficking mutants on the expression and maturation of WT, as well as the physical interactions between mutant-WT subunits.

The N-linker mutant G306W is a mild trafficking mutant, which did not cause any changes in WT maturation when co-expressed, and showed an association with WT subunits comparable to that of WT-WT. Of note, G306W has not been previously characterized biophysically, thus the gating properties of this mutant remains unknown. Should it display any gating defects, it then has the possibility of being a functional DN mutant.

Both pore mutants G601S and A561V impaired trafficking of WT subunits, demonstrated by the reduction of WT FG bands upon co-expression. WT also mildly promoted G601S maturation, suggesting heteromerization between mutant and WT subunits, and potential forward trafficking of the heteromers. Co-IP results confirmed the formation of mutant-WT mixed-tetramers, which were largely retained in the ER, with a small post Golgi fraction. However, it is unclear whether the heteromer would be functional if trafficked to the cell membrane or would even accumulate a significant channel population on the cell membrane. Overall, our data suggests that A561V and G601S exerted a DN effect on WT subunits, and is consistent with the

available literature (76,95,98,108). Patch clamp experiments were performed in two previous studies on A561V-WT heteromers, which showed marked suppression of hERG currents, consistent with it being dominant negative (76,98). Surprisingly, for G601S, there has been one previous electrophysiology study which reported no dominant-negative effect on WT subunits. However, the conclusion was based on patch clamp experiments done in *Xenopus* oocyte, and at 23 °C (110). Given the known effect of temperature on the trafficking of many hERG mutants, and the variations in the cellular processing system between *Xenopus* and humans, it is uncertain whether the phenotype would be reproducible in human cell lines.

The two CNBHD mutants F805C and G816V had no significant effect on WT subunit maturation and processing, suggesting they follow a HI mechanism. However, both mutants showed significant CG interactions with WT. This finding is inconsistent with HI where one should expect that mutants do not co-assemble with WT subunits, sparing them from ER retention and degradation. However, both mutants displayed decreased CG interaction and minimal FG interactions with WT subunits, suggesting overall reduced interactions, and minimal mutant involvement in the functional channel on the cell surface. Our data agrees with a previous study by Krishnan et al. (96) who also observed significant CG interactions between WT and G816V, despite immunoblot and patch clamp data suggesting a non-dominant mechanism. However for F805C, two previous heteromeric screens produced conflicting results. A 2006 study carried out with transient co-transfections in HEK 293 cells and manual patch clamp showed around 50% reduction in current for WT-F805C heteromers, consistent with a HI mechanism (88). However, a 2019 study detected minimal (<20%) current produced by the F805C-WT heteromers, through the inducible expression of a WT-F805C bi-cistronic construct in a Flp-In HEK293 cell line, using high-throughput automated patch clamp (98). The

discrepancy between the studies could possibly be attributed to the variations in experimental systems and patch clamp techniques.

There are a few potential explanations for the observed CG interactions between WT and the proposed HI mutants. It is well known that when hERG is expressed heterologously, it accumulates significantly in the ER, resulting in a strong CG band. This CG band is resistant to degradation and forward-trafficking, with little appreciable changes observed following 6 hours of translation inhibition by cycloheximide (70). Perhaps HI mutants can still associate with WT in the CG form, but to a much lesser degree so that it does not significantly affect the abundance of WT homomers and their trafficking. It is also possible that WT and F805C or G816V subunits do not interact with each other in the initial assembly of the tetramers, but only dynamically exchange subunits into heteromers during the long accumulation at the ER. Secondly, even though this study sorted mutants into DN or HI mechanisms, it is in fact very likely that these two categories only serve as two ends of a spectrum, with most mutants showing intermediate, mutant-specific phenotypes with DN or HI tendencies. Lastly, even though the most common mechanism underlying mutant dominance is via co-assembly with WT subunits, it is still possible that other mechanisms can contribute to it. Severely misfolded proteins could potentially cause non-specific disruption of the protein transport pathway, thus resulting in aberrant trafficking of other proteins sharing the pathway (59,115). This has been observed for severely misfolded growth hormone, which altered the structure and integrity of the Golgi apparatus, causing a generalized impairment in ER-Golgi transfer of other protein clients (59,115).

There are several limitations in this study. First is the lack of electrophysiological data on the mutant-WT heteromers. Without functional assessment, it would be difficult to determine

whether mutants are in fact consistent with a dominant negative or haploinsufficiency mechanism. The second potential limitation is the use of a heterologous system. hERG is endogenously expressed in cardiomyocytes, which may contain cardiac or muscle-specific traits in its intracellular signaling and in protein synthesis/trafficking pathways. In addition, the use of a heterologous system to study hERG 1a-1b WT heteromers is challenging because it involves complex co-transfections of multiple plasmids for each mutant, and thus was not conducted in this study. The final limitation is the relatively small number of mutants assessed, which limits the ability to draw correlations between the location of mutation in the hERG domains and the severities of the phenotype. Mutants from the PAS and the S1-S4 domains were not explored, which would be the subject for future study. Nevertheless, the approaches used in this thesis combined with patch clamp analysis, can be used to address further hERG mutants. Other methods such as cell surface ELISA (85) and localization of hERG channels by imaging could provide additional support to the conclusions.

## **Material and methods:**

# Recombinant DNA constructs and mutagenesis

Wild type, G601S and F805C hERG in vector pcDNA3.1, with HA (YPYDVPDYA) epitope tag inserted between the S1-S2 loop of hERG (after aa.433) was a gift from Eckhard Ficker (68). Using WT hERG pcDNA3.1 as a template, point mutations A561V, G816V and G306W were introduced via overlap extension PCR, and inserted between intrinsic sites *BamHI-PasI* (G306W), *PasI-SbfI* (A561V) and *SbfI-FseI* (G816V). In addition, WT hERG-pcDNA 3.1 with myc (EQKLISEEDL) epitope tag, inserted at the same location as the HA tag, was generated by Bio Basic Inc. All constructs were sequenced routinely to ensure no spontaneous mutations were introduced during PCRs or through the bacterial DNA replication system. WT KCNQ4 in pCMV-XL5 vector, with N-terminal myc or HA epitope tags were obtained from the Young lab.

### Tissue culture

Parental HeLa cells (ATCC) were cultured on polystyrene coated 100mm plates (Corning), in HEPA filtered incubators, with humidified air at 37 °C, and 5% ambient CO<sub>2</sub>. Cells are maintained in Dulbecco's Modified Eagle Medium (DMEM), with glucose, L-glutamine and sodium pyruvate (Wisent), supplemented with 10% of fetal bovine serum (FBS)(Wisent), 100 unit/mL Penicillin and 100 μg/mL Streptomycin (Wisent). Regular mycoplasma and CO<sub>2</sub> testing were conducted to ensure the quality of the cell cultures.

#### **Transient transfection**

WT and mutant plasmids were co-transfected into parental HeLa cells at a confluence of 60-80%. HeLa cells were first plated on polystyrene coated 6 well plate (Corning). After 24 hours, 1 µg WT<sub>myc</sub> hERG with either 1 µg of mutantha hERG or WTha hERG, or control ion channel KCNQ4<sub>HA</sub>, or mutantha (or WTha) with KCNQ4<sub>myc</sub> were transiently co-transfected into

the cells. Transfections were performed using Fugene 6 (Promega) according to manufacturer's instructions. For every μg of DNA, 3 μL of Fugene 6 was used. Briefly, DNA combinations were first mixed in DMEM. Corresponding amount of Fugene 6 was also mixed with DMEM in a separate Eppendorf tube and incubated at 5 minutes at room temperature (RT). After, DNA and Fugene 6 mixtures were combined and incubated at RT for 15 minutes. During this incubation, cells were washed with PBS and replaced with DMEM containing 10% FBS. After 15 minutes, the Fugene-DNA mixture were added to the cells dropwise, and incubated for 5 hours at 37 °C. The transfection media were replaced with growth media (DMEM+FBS + antibiotics), and cells were split at a 1:2 ratio to avoid over-confluence and incubated at 37 °C for 43 hours before harvest. For IP experiments, transfections were performed on 100 mm polystyrene dishes (Corning), with 8 μg of total DNA. For drug treatment, cells at 24 hours post transfection was incubated with either 0.1μM of Thapsigargin, or with equivalent volume of DMSO (solvent) for 24 hours. Thapsigargin and DMSO obtained from the Young lab.

#### Western Blot

Cells were first washed 2 x with cooled phosphate-buffered saline (PBS), and then collected in 1 mL PBS into Eppendorf tubes with a scrapper. Then samples were centrifuged at 1000 xg for 5 minutes at 4 °C. After, supernatant was then aspirated, and pellet was lysed by resuspending in 100 μL of ice cold lysis buffer (PBS + 1% Triton X-100, and 1 EDTA free protease inhibitor cocktail tablet (Roche)). After incubation on ice for 10 minutes, cells were centrifuged at 16,000 xg at 4 °C for 5 minutes, to collect the cell lysate in the supernatant. The protein concentration of each lysate was determined using the BioRad DC<sup>TM</sup> Protein Assay Kit, and concentration values obtained through absorbance/concentration plot generated by serial dilutions of freshly prepared 10 μg/μL BSA solutions. Then, lysate concentrations were

equalized with lysis buffer, and Laemmli loading buffer (0.1 M Tris pH 6.8, 10% glycerol, 10% SDS, 10% 2-Mercaptoethanol) were added to each sample at a 1:1 ratio. Samples were then mixed and incubated on heat block of 60 °C for 15 minutes. Proteins on the samples where then separated by 7% acrylamide sodium dodecyl sulfate poly acrylamide gel electrophoresis (SDS PAGE). After, proteins were electrically transferred onto nitrocellulose membrane with pore size of 0.45 μm (GE healthcare), overnight at 50 mA, in transfer buffer (500 mM Glycine, 50 mM Tris-HCl, 0.01% SDS, 2 0% Ethanol).

Transferred membranes were blocked with either 5% skim milk (for monoclonal antibodies), or 5% BSA (for polyclonal antibodies) in PBS supplemented with 0.1% Tween-20 (PBS-T) at RT for 30 minutes. Then membranes were incubated with one of the following antibodies: anti-myc, anti-HA, anti-Tubulin, anti-BiP or anti-hERG, in the respective blocking condition for either 2 hours at RT, or at 4 °C overnight, under constant gentle shaking.

Membranes were then washed 3 times, 5 minutes each, by PBS-T. Secondary antibodies incubation performed with either goat anti-mouse IgG conjugated to horseradish peroxidase (HRP) (Jackson ImmunoResearch), or goat anti-rabbit IgG conjugated to HRP (Jackson ImmunoResearch), at a dilution of 1:5000 in their perspective blocking solutions, and subsequently washed again 3 times of 5 minutes each, in PBS-T. Finally, signal development was carried out with ECL blotting detection reagents (GE Healthcare) and captured using a FluorChem HD2 digital camera (Alpha Innotech).

## **Co-immunoprecipitation (Co-IP)**

48 hours prior to co-IP, HeLa cells were plated on 100 mm polystyrene coated dishes and transfected with WT and mutant hERG plasmid combinations as described above. At time of harvest, cells were lysed in a similar manner as for western blots, but in 500 µL PBS + 0.1%

Triton-X buffer and 1 tablet of protease inhibitor (mini). After lysate normalization, 50 µl of lysates were taken out as input control, mixed at a 1:1 ratio with Laemmli loading buffer and the remaining mixed with 30 µL magnetic beads conjugated with either anti-myc or anti-HA antibodies (Pierce Thermofisher). Samples were then incubated at 4 °C overnight, with gentle rocking. After incubation, the beads were washed 5 times with ice cold lysis buffer. Lastly, elution was carried out by resuspending magnetic beads in 60 µL Laemmli buffer (without 2-mercaptoethanol) and incubation at 72 °C for 10 minutes with gentle mixing. Magnetic beads were separated from the elutes by using a magnetic stand. 2-mercaptoethanol was then added to the samples to reach a final concentration of 10%. Rest of the procedures, including heat block, SDS PAGE, antibody incubation and signal detection were as described above for western blots.

#### **Antibodies**

For western blots, mouse monoclonal anti-myc antibody (9E10) 1:1000 was obtained from Abcam. For Co-IP, mouse monoclonal anti-myc antibody (9E10) 1:250 was obtained from Invitrogen. Rabbit polyclonal anti-Kv11.1 (hERG) antibody 1:2000 was obtained from Alomone. Mouse monoclonal anti-HA (HA-11) antibody 1:1000 was obtained from Biolegend. Mouse monoclonal anti-tubulin 1:30000 antibody was obtained from Sigma-Aldrich. Goat anti-rabbit IgG conjugated HRP 1:5000 antibody, and goat anti-mouse IgG conjugated HRP 1:5000 were obtained from Jackson Immunoresearch. Anti-BiP antibody was a gift from the David Thomas lab.

### **Blot analysis and statistics**

Immunoblot images were analyzed using Image J (National Institutes of Health, version 2.00 (8-bit), Bethesda, MD) to measure the relative density of protein amount with respect to control samples. Graphs were generated via Prism 8 GraphPad and Ms Excel. Each experiment

was repeated for at least 3 times (n>3), and the statistical significance of the results was analyzed by unpaired, two-tailed student's t-test, with  $p \le 0.05$  set as the significance threshold. Error bars denote standard error of the mean.

# Reference

- 1. Ackerman, M. J., Schwartz, P. J., and Asirvatham, S. (2019) Congenital long QT syndrome: Pathophysiology and genetics. in *UpToDate*https://www.uptodate.com/contents/congenital-long-qt-syndrome-pathophysiology-and-genetics (Triedman, J., Asirvatham, S., and Downey, B. eds.), Waltham, MA.
- 2. Shah, S. R., Park, K., and Alweis, R. (2019) Long QT syndrome: a comprehensive review of the literature and current evidence. *Current problems in cardiology* **44**, 92-106
- 3. Nakano, Y., and Shimizu, W. (2016) Genetics of long-QT syndrome. *Journal of human genetics* **61**, 51-55
- 4. Crotti, L., Celano, G., Dagradi, F., and Schwartz, P. J. (2008) Congenital long QT syndrome. *Orphanet journal of rare diseases* **3**, 18
- 5. Stramba-Badiale, M., Crotti, L., Goulene, K., Pedrazzini, M., Mannarino, S., Salice, P., Bosi, G., Nespoli, L., Rimini, A., and Gabbarini, F. (2007) Electrocardiographic and genetic screening for long QT syndrome: results from a prospective study on 44,596 neonates. Am Heart Assoc
- 6. Berul, C. (2018) Acquired long QT syndrome: Definitions, causes, and pathophysiology. in *UpToDate https://www.uptodate.com/contents/acquired-long-qt-syndrome-definitions-causes-and-pathophysiology* (Asirvatham, S., Zimetbaum, P., Downey, B. eds.), Waltham, MA.
- 7. Kang, J., Wang, L., Chen, X.-L., Triggle, D. J., and Rampe, D. (2001) Interactions of a series of fluoroquinolone antibacterial drugs with the human cardiac K+ channel HERG. *Molecular pharmacology* **59**, 122-126
- 8. Suessbrich, H., Schönherr, R., Heinemann, S., Attali, B., Lang, F., and Busch, A. (1997) The inhibitory effect of the antipsychotic drug haloperidol on HERG potassium channels expressed in Xenopus oocytes. *British journal of pharmacology* **120**, 968-974
- 9. Hancox, J. C., McPate, M. J., El Harchi, A., and hong Zhang, Y. (2008) The hERG potassium channel and hERG screening for drug-induced torsades de pointes. *Pharmacology & therapeutics* **119**, 118-132
- 10. Ackerman, M. J., Schwartz, P. J., and Asirvatham, S. Congenital long QT syndrome: Pathophysiology and genetics.
- 11. Shojaie, M., and Eshraghian, A. (2008) Primary hypothyroidism presenting with Torsades de pointes type tachycardia: a case report. *Cases journal* 1, 298
- 12. Ali, R. H. H., Zareba, W., Moss, A. J., Schwartz, P. J., Benhorin, J., Vincent, G. M., Locati, E. H., Priori, S., Napolitano, C., and Towbin, J. A. (2000) Clinical and genetic variables associated with acute arousal and nonarousal-related cardiac events among subjects with the long QT syndrome. *The American journal of cardiology* **85**, 457-461
- 13. Al-Khatib, S. M., Stevenson, W. G., Ackerman, M. J., Bryant, W. J., Callans, D. J., Curtis, A. B., Deal, B. J., Dickfeld, T., Field, M. E., and Fonarow, G. C. (2018) 2017 AHA/ACC/HRS guideline for management of patients with ventricular arrhythmias and the prevention of sudden cardiac death: a report of the American College of Cardiology/American Heart Association Task Force on Clinical Practice Guidelines and the Heart Rhythm Society. *Journal of the American College of Cardiology* 72, e91-e220
- 14. Bohnen, M., Peng, G., Robey, S., Terrenoire, C., Iyer, V., Sampson, K., and Kass, R. (2017) Molecular pathophysiology of congenital long QT syndrome. *Physiological reviews* **97**, 89-134

- 15. Jost, N. (2009) Transmembrane ionic currents underlying cardiac action potential in mammalian hearts. *Advances in cardiomyocyte research. Ed. Péter P. Nánási. Transworld Research Network, Tivandrum, Kerala, India*, 1-45
- 16. Kalyaanamoorthy, S., and Barakat, K. H. (2018) Development of safe drugs: the hERG challenge. *Medicinal research reviews* **38**, 525-555
- 17. Fermini, B., and Fossa, A. A. (2003) The impact of drug-induced QT interval prolongation on drug discovery and development. *Nat Rev Drug Discov* **2**, 439-447
- 18. Huang, H., Pugsley, M. K., Fermini, B., Curtis, M. J., Koerner, J., Accardi, M., and Authier, S. (2017) Cardiac voltage-gated ion channels in safety pharmacology: Review of the landscape leading to the CiPA initiative. *J Pharmacol Toxicol Methods* **87**, 11-23
- 19. Vandenberg, J. I., Perry, M. D., Perrin, M. J., Mann, S. A., Ke, Y., and Hill, A. P. (2012) hERG K+ channels: structure, function, and clinical significance. *Physiological reviews* **92**, 1393-1478
- 20. Anantharam, A., and Abbott, G. W. (2005) Does hERG coassemble with a β subunit? Evidence for roles of MinK and MiRP1. in *The hERG Cardiac Potassium Channel: Structure, Function and Long QT Syndrome: Novartis Foundation Symposium 266*, Wiley Online Library
- 21. Kim, D. G., Oh, J. H., Lee, E. H., Lee, J. H., Park, H. J., Kim, C. Y., Kwon, M. S., and Yoon, S. (2010) The stoichiometric relationship between KCNH-2 and KCNE-2 in I(Kr) channel formation. *Int J Cardiol* **145**, 272-274
- 22. Mazhari, R., Greenstein, J. L., Winslow, R. L., Marbán, E., and Nuss, H. B. (2001) Molecular interactions between two long-QT syndrome gene products, HERG and KCNE2, rationalized by in vitro and in silico analysis. *Circulation research* **89**, 33-38
- 23. Um, S. Y., and McDonald, T. V. (2007) Differential association between HERG and KCNE1 or KCNE2. *PloS one* **2**
- 24. Wang, W., and MacKinnon, R. (2017) Cryo-EM structure of the open human ether-à-go-go-related K+ channel hERG. *Cell* **169**, 422-430. e410
- 25. Jones, D. K., Liu, F., Vaidyanathan, R., Eckhardt, L. L., Trudeau, M. C., and Robertson, G. A. (2014) hERG 1b is critical for human cardiac repolarization. *Proceedings of the National Academy of Sciences* 111, 18073-18077
- 26. Jones, E. M., Roti, E. C. R., Wang, J., Delfosse, S. A., and Robertson, G. A. (2004) Cardiac IKr channels minimally comprise hERG 1a and 1b subunits. *Journal of Biological Chemistry* **279**, 44690-44694
- 27. Foo, B., Williamson, B., Young, J. C., Lukacs, G., and Shrier, A. (2016) hERG quality control and the long QT syndrome. *The Journal of physiology* **594**, 2469-2481
- 28. Perissinotti, L. L., De Biase, P. M., Guo, J., Yang, P.-C., Lee, M. C., Clancy, C. E., Duff, H. J., and Noskov, S. Y. (2018) Determinants of isoform-specific gating kinetics of hERG1 channel: combined experimental and simulation study. *Frontiers in physiology* 9, 207
- 29. Phartiyal, P., Jones, E. M., and Robertson, G. A. (2007) Heteromeric assembly of human ether-a-go-go-related gene (hERG) 1a/1b channels occurs cotranslationally via N-terminal interactions. *Journal of Biological Chemistry* **282**, 9874-9882
- 30. Phartiyal, P., Sale, H., Jones, E. M., and Robertson, G. A. (2008) Endoplasmic reticulum retention and rescue by heteromeric assembly regulate human ERG 1a/1b surface channel composition. *Journal of Biological Chemistry* **283**, 3702-3707

- 31. Puckerin, A., Aromolaran, K. A., Chang, D. D., Zukin, R. S., Colecraft, H. M., Boutjdir, M., and Aromolaran, A. S. (2016) hERG 1a LQT2 C-terminus truncation mutants display hERG 1b-dependent dominant negative mechanisms. *Heart Rhythm* 13, 1121-1130
- 32. Sale, H., Wang, J., O'Hara, T. J., Tester, D. J., Phartiyal, P., He, J.-Q., Rudy, Y., Ackerman, M. J., and Robertson, G. A. (2008) Physiological properties of hERG 1a/1b heteromeric currents and a hERG 1b-specific mutation associated with Long-QT syndrome. *Circulation research* **103**, e81-e95
- 33. Sanguinetti, M. C., Jiang, C., Curran, M. E., and Keating, M. T. (1995) A mechanistic link between an inherited and an acquird cardiac arrthytmia: HERG encodes the IKr potassium channel. *Cell* **81**, 299-307
- 34. Wang, S., Liu, S., Morales, M. J., Strauss, H. C., and Rasmusson, R. L. (1997) A quantitative analysis of the activation and inactivation kinetics of HERG expressed in Xenopus oocytes. *The Journal of Physiology* **502**, 45-60
- 35. Liu, F., Jones, D. K., de Lange, W. J., and Robertson, G. A. (2016) Cotranslational association of mRNA encoding subunits of heteromeric ion channels. *Proceedings of the National Academy of Sciences* **113**, 4859-4864
- 36. Sanguinetti, M. C., and Tristani-Firouzi, M. (2006) hERG potassium channels and cardiac arrhythmia. *Nature* **440**, 463-469
- 37. Perry, M., Sanguinetti, M., and Mitcheson, J. (2010) Symposium review: Revealing the structural basis of action of hERG potassium channel activators and blockers. *The Journal of physiology* **588**, 3157-3167
- 38. Robertson, G. A., and Morais-Cabral, J. H. (2020) hERG function in light of structure. *Biophysical journal* **118**, 790-797
- 39. Cabral, J. H. M., Lee, A., Cohen, S. L., Chait, B. T., Li, M., and Mackinnon, R. (1998) Crystal structure and functional analysis of the HERG potassium channel N terminus: a eukaryotic PAS domain. *Cell* **95**, 649-655
- 40. Warmke, J. W., and Ganetzky, B. (1994) A family of potassium channel genes related to eag in Drosophila and mammals. *Proceedings of the National Academy of Sciences* **91**, 3438-3442
- 41. Tang, X., Shao, J., and Qin, X. (2016) Crystal structure of the PAS domain of the hEAG potassium channel. *Acta Crystallogr F Struct Biol Commun* **72**, 578-585
- 42. Chen, J., Zou, A., Splawski, I., Keating, M. T., and Sanguinetti, M. C. (1999) Long QT syndrome-associated mutations in the Per-Arnt-Sim (PAS) domain of HERG potassium channels accelerate channel deactivation. *J Biol Chem* **274**, 10113-10118
- 43. Gustina, A. S., and Trudeau, M. C. (2013) The eag domain regulates hERG channel inactivation gating via a direct interaction. *J Gen Physiol* **141**, 229-241
- 44. Liu, Q. N., and Trudeau, M. C. (2015) Eag Domains Regulate LQT Mutant hERG Channels in Human Induced Pluripotent Stem Cell-Derived Cardiomyocytes. *PLoS One* **10**, e0123951
- 45. Gustina, A. S., and Trudeau, M. C. (2009) A recombinant N-terminal domain fully restores deactivation gating in N-truncated and long QT syndrome mutant hERG potassium channels. *Proc Natl Acad Sci U S A* **106**, 13082-13087
- 46. Ke, Y., Ng, C. A., Hunter, M. J., Mann, S. A., Heide, J., Hill, A. P., and Vandenberg, J. I. (2013) Trafficking defects in PAS domain mutant Kv11.1 channels: roles of reduced domain stability and altered domain-domain interactions. *Biochem J* **454**, 69-77

- 47. Ng, C. A., Hunter, M. J., Perry, M. D., Mobli, M., Ke, Y., Kuchel, P. W., King, G. F., Stock, D., and Vandenberg, J. I. (2011) The N-terminal tail of hERG contains an amphipathic α-helix that regulates channel deactivation. *PLoS One* **6**, e16191
- 48. Ng, C. A., Phan, K., Hill, A. P., Vandenberg, J. I., and Perry, M. D. (2014) Multiple interactions between cytoplasmic domains regulate slow deactivation of Kv11.1 channels. *J Biol Chem* **289**, 25822-25832
- 49. Gianulis, E. C., Liu, Q., and Trudeau, M. C. (2013) Direct interaction of eag domains and cyclic nucleotide-binding homology domains regulate deactivation gating in hERG channels. *J Gen Physiol* **142**, 351-366
- 50. Li, Q., Gayen, S., Chen, A. S., Huang, Q., Raida, M., and Kang, C. (2010) NMR solution structure of the N-terminal domain of hERG and its interaction with the S4-S5 linker. *Biochem Biophys Res Commun* **403**, 126-132
- 51. Ron, D., and Walter, P. (2007) Signal integration in the endoplasmic reticulum unfolded protein response. *Nat Rev Mol Cell Biol* **8**, 519-529
- 52. Brelidze, T. I., Carlson, A. E., and Zagotta, W. N. (2009) Absence of direct cyclic nucleotide modulation of mEAG1 and hERG1 channels revealed with fluorescence and electrophysiological methods. *J Biol Chem* **284**, 27989-27997
- 53. Li, Q., Ng, H. Q., Yoon, H. S., and Kang, C. (2014) Insight into the molecular interaction between the cyclic nucleotide-binding homology domain and the eag domain of the hERG channel. *FEBS Lett* **588**, 2782-2788
- 54. Li, Y., Ng, H. Q., Li, Q., and Kang, C. (2016) Structure of the Cyclic Nucleotide-Binding Homology Domain of the hERG Channel and Its Insight into Type 2 Long QT Syndrome. *Sci Rep* **6**, 23712
- 55. Codding, S. J., and Trudeau, M. C. (2019) The hERG potassium channel intrinsic ligand regulates N- and C-terminal interactions and channel closure. *J Gen Physiol* **151**, 478-488
- 56. Akhavan, A., Atanasiu, R., Noguchi, T., Han, W., Holder, N., and Shrier, A. (2005) Identification of the cyclic-nucleotide-binding domain as a conserved determinant of ion-channel cell-surface localization. *J Cell Sci* **118**, 2803-2812
- 57. Akhavan, A., Atanasiu, R., and Shrier, A. (2003) Identification of a COOH-terminal segment involved in maturation and stability of human ether-a-go-go-related gene potassium channels. *J Biol Chem* **278**, 40105-40112
- 58. Gong, Q., Anderson, C. L., January, C. T., and Zhou, Z. (2004) Pharmacological rescue of trafficking defective HERG channels formed by coassembly of wild-type and long QT mutant N470D subunits. *Am J Physiol Heart Circ Physiol* **287**, H652-658
- 59. Gong, Q., Keeney, D. R., Robinson, J. C., and Zhou, Z. (2004) Defective assembly and trafficking of mutant HERG channels with C-terminal truncations in long QT syndrome. *J Mol Cell Cardiol* 37, 1225-1233
- 60. Kupershmidt, S., Yang, T., Chanthaphaychith, S., Wang, Z., Towbin, J. A., and Roden, D. M. (2002) Defective human Ether-à-go-go-related gene trafficking linked to an endoplasmic reticulum retention signal in the C terminus. *J Biol Chem* **277**, 27442-27448
- 61. Jenke, M., Sánchez, A., Monje, F., Stühmer, W., Weseloh, R. M., and Pardo, L. A. (2003) C-terminal domains implicated in the functional surface expression of potassium channels. *Embo j* **22**, 395-403
- 62. Choe, C. U., Schulze-Bahr, E., Neu, A., Xu, J., Zhu, Z. I., Sauter, K., Bähring, R., Priori, S., Guicheney, P., Mönnig, G., Neapolitano, C., Heidemann, J., Clancy, C. E., Pongs, O.,

- and Isbrandt, D. (2006) C-terminal HERG (LQT2) mutations disrupt IKr channel regulation through 14-3-3epsilon. *Hum Mol Genet* **15**, 2888-2902
- 63. Lin, T. F., Lin, I. W., Chen, S. C., Wu, H. H., Yang, C. S., Fang, H. Y., Chiu, M. M., and Jeng, C. J. (2014) The subfamily-specific assembly of Eag and Erg K+ channels is determined by both the amino and the carboxyl recognition domains. *J Biol Chem* **289**, 22815-22834
- 64. Gong, Q., Anderson, C. L., January, C. T., and Zhou, Z. (2002) Role of glycosylation in cell surface expression and stability of HERG potassium channels. *Am J Physiol Heart Circ Physiol* **283**, H77-84
- 65. Delisle, B. P., Underkofler, H. A., Moungey, B. M., Slind, J. K., Kilby, J. A., Best, J. M., Foell, J. D., Balijepalli, R. C., Kamp, T. J., and January, C. T. (2009) Small GTPase determinants for the Golgi processing and plasmalemmal expression of human etherago-go related (hERG) K+ channels. *J Biol Chem* **284**, 2844-2853
- 66. Lamothe, S. M., Hulbert, M., Guo, J., Li, W., Yang, T., and Zhang, S. (2018) Glycosylation stabilizes hERG channels on the plasma membrane by decreasing proteolytic susceptibility. *Faseb j* **32**, 1933-1943
- 67. Foo, B., Barbier, C., Guo, K., Vasantharuban, J., Lukacs, G. L., and Shrier, A. (2019) Mutation-specific peripheral and ER quality control of hERG channel cell-surface expression. *Sci Rep* **9**, 6066
- 68. Ficker, E., Dennis, A. T., Wang, L., and Brown, A. M. (2003) Role of the cytosolic chaperones Hsp70 and Hsp90 in maturation of the cardiac potassium channel HERG. *Circ Res* **92**, e87-100
- 69. Walker, V. E., Atanasiu, R., Lam, H., and Shrier, A. (2007) Co-chaperone FKBP38 promotes HERG trafficking. *J Biol Chem* **282**, 23509-23516
- 70. Hantouche, C., Williamson, B., Valinsky, W. C., Solomon, J., Shrier, A., and Young, J. C. (2017) Bag1 Co-chaperone Promotes TRC8 E3 Ligase-dependent Degradation of Misfolded Human Ether a Go-Go-related Gene (hERG) Potassium Channels. *J Biol Chem* **292**, 2287-2300
- 71. Young, J. C. (2014) The role of the cytosolic HSP70 chaperone system in diseases caused by misfolding and aberrant trafficking of ion channels. *Dis Model Mech* 7, 319-329
- 72. Li, P., Ninomiya, H., Kurata, Y., Kato, M., Miake, J., Yamamoto, Y., Igawa, O., Nakai, A., Higaki, K., Toyoda, F., Wu, J., Horie, M., Matsuura, H., Yoshida, A., Shirayoshi, Y., Hiraoka, M., and Hisatome, I. (2011) Reciprocal control of hERG stability by Hsp70 and Hsc70 with implication for restoration of LQT2 mutant stability. *Circ Res* **108**, 458-468
- 73. Walker, V. E., Wong, M. J., Atanasiu, R., Hantouche, C., Young, J. C., and Shrier, A. (2010) Hsp40 chaperones promote degradation of the HERG potassium channel. *J Biol Chem* **285**, 3319-3329
- 74. Li, J., Soroka, J., and Buchner, J. (2012) The Hsp90 chaperone machinery: conformational dynamics and regulation by co-chaperones. *Biochim Biophys Acta* **1823**, 624-635
- 75. Iwai, C., Li, P., Kurata, Y., Hoshikawa, Y., Morikawa, K., Maharani, N., Higaki, K., Sasano, T., Notsu, T., Ishido, Y., Miake, J., Yamamoto, Y., Shirayoshi, Y., Ninomiya, H., Nakai, A., Murata, S., Yoshida, A., Yamamoto, K., Hiraoka, M., and Hisatome, I. (2013) Hsp90 prevents interaction between CHIP and HERG proteins to facilitate maturation of wild-type and mutant HERG proteins. *Cardiovasc Res* **100**, 520-528

- 76. Kagan, A., Yu, Z., Fishman, G. I., and McDonald, T. V. (2000) The dominant negative LQT2 mutation A561V reduces wild-type HERG expression. *J Biol Chem* **275**, 11241-11248
- 77. Ludwig, J., Owen, D., and Pongs, O. (1997) Carboxy-terminal domain mediates assembly of the voltage-gated rat ether-à-go-go potassium channel. *Embo j* **16**, 6337-6345
- 78. Li, X., Xu, J., and Li, M. (1997) The human delta1261 mutation of the HERG potassium channel results in a truncated protein that contains a subunit interaction domain and decreases the channel expression. *J Biol Chem* **272**, 705-708
- 79. Matsumura, Y., Sakai, J., and Skach, W. R. (2013) Endoplasmic reticulum protein quality control is determined by cooperative interactions between Hsp/c70 protein and the CHIP E3 ligase. *J Biol Chem* **288**, 31069-31079
- 80. Roder, K., Kabakov, A., Moshal, K. S., Murphy, K. R., Xie, A., Dudley, S., Turan, N. N., Lu, Y., MacRae, C. A., and Koren, G. (2019) Trafficking of the human ether-a-go-go-related gene (hERG) potassium channel is regulated by the ubiquitin ligase rififylin (RFFL). *J Biol Chem* **294**, 351-360
- 81. Guo, K. (2018) Retrotranslocation of the human ether-a-go-go related gene (hERG) potassium channel and its Long QT Syndrome (LQTS) causing mutants Master's thesis McGill University
- 82. Stach, L., and Freemont, P. S. (2017) The AAA+ ATPase p97, a cellular multitool. *Biochem J* **474**, 2953-2976
- 83. Tanaka, K. (2009) The proteasome: overview of structure and functions. *Proc Jpn Acad Ser B Phys Biol Sci* **85**, 12-36
- 84. Kang, Y., Guo, J., Yang, T., Li, W., and Zhang, S. (2015) Regulation of the human ethera-go-go-related gene (hERG) potassium channel by Nedd4 family interacting proteins (Ndfips). *Biochem J* **472**, 71-82
- 85. Apaja, P. M., Foo, B., Okiyoneda, T., Valinsky, W. C., Barriere, H., Atanasiu, R., Ficker, E., Lukacs, G. L., and Shrier, A. (2013) Ubiquitination-dependent quality control of hERG K+ channel with acquired and inherited conformational defect at the plasma membrane. *Mol Biol Cell* **24**, 3787-3804
- 86. Schulze, H., Kolter, T., and Sandhoff, K. (2009) Principles of lysosomal membrane degradation: Cellular topology and biochemistry of lysosomal lipid degradation. *Biochim Biophys Acta* **1793**, 674-683
- 87. Anderson, C. L., Kuzmicki, C. E., Childs, R. R., Hintz, C. J., Delisle, B. P., and January, C. T. (2014) Large-scale mutational analysis of Kv11. 1 reveals molecular insights into type 2 long QT syndrome. *Nature communications* 5, 1-13
- 88. Anderson, C. L., Delisle, B. P., Anson, B. D., Kilby, J. A., Will, M. L., Tester, D. J., Gong, Q., Zhou, Z., Ackerman, M. J., and January, C. T. (2006) Most LQT2 mutations reduce Kv11.1 (hERG) current by a class 2 (trafficking-deficient) mechanism. *Circulation* 113, 365-373
- 89. Zhou, Z., Gong, Q., and January, C. T. (1999) Correction of defective protein trafficking of a mutant HERG potassium channel in human long QT syndrome. Pharmacological and temperature effects. *J Biol Chem* **274**, 31123-31126
- 90. Moss, A. J., Zareba, W., Kaufman, E. S., Gartman, E., Peterson, D. R., Benhorin, J., Towbin, J. A., Keating, M. T., Priori, S. G., Schwartz, P. J., Vincent, G. M., Robinson, J. L., Andrews, M. L., Feng, C., Hall, W. J., Medina, A., Zhang, L., and Wang, Z. (2002)

- Increased risk of arrhythmic events in long-QT syndrome with mutations in the pore region of the human ether-a-go-go-related gene potassium channel. *Circulation* **105**, 794-799
- 91. Sottas, V., and Abriel, H. (2016) Negative-dominance phenomenon with genetic variants of the cardiac sodium channel Nav1. 5. *Biochimica et Biophysica Acta (BBA)-Molecular Cell Research* **1863**, 1791-1798
- 92. Moss, A. J., Shimizu, W., Wilde, A. A., Towbin, J. A., Zareba, W., Robinson, J. L., Qi, M., Vincent, G. M., Ackerman, M. J., Kaufman, E. S., Hofman, N., Seth, R., Kamakura, S., Miyamoto, Y., Goldenberg, I., Andrews, M. L., and McNitt, S. (2007) Clinical aspects of type-1 long-QT syndrome by location, coding type, and biophysical function of mutations involving the KCNQ1 gene. *Circulation* 115, 2481-2489
- 93. Huo, J., Zhang, Y., Huang, N., Liu, P., Huang, C., Guo, X., Jiang, W., Zhou, N., Grace, A., Huang, C. L., and Ma, A. (2008) The G604S-hERG mutation alters the biophysical properties and exerts a dominant-negative effect on expression of hERG channels in HEK293 cells. *Pflugers Arch* **456**, 917-928
- 94. Aidery, P., Kisselbach, J., Gaspar, H., Baldea, I., Schweizer, P. A., Becker, R., Katus, H. A., and Thomas, D. (2012) Identification and functional characterization of the novel human ether-a-go-go-related gene (hERG) R744P mutant associated with hereditary long QT syndrome 2. *Biochem Biophys Res Commun* **418**, 830-835
- 95. Ficker, E., Dennis, A. T., Obejero-Paz, C. A., Castaldo, P., Taglialatela, M., and Brown, A. M. (2000) Retention in the endoplasmic reticulum as a mechanism of dominant-negative current suppression in human long QT syndrome. *J Mol Cell Cardiol* **32**, 2327-2337
- 96. Krishnan, Y., Zheng, R., Walsh, C., Tang, Y., and McDonald, T. V. (2012) Partially dominant mutant channel defect corresponding with intermediate LQT2 phenotype. *Pacing Clin Electrophysiol* **35**, 3-16
- 97. Zhao, J. T., Hill, A. P., Varghese, A., Cooper, A. A., Swan, H., Laitinen-Forsblom, P. J., Rees, M. I., Skinner, J. R., Campbell, T. J., and Vandenberg, J. I. (2009) Not all hERG pore domain mutations have a severe phenotype: G584S has an inactivation gating defect with mild phenotype compared to G572S, which has a dominant negative trafficking defect and a severe phenotype. *J Cardiovasc Electrophysiol* **20**, 923-930
- 98. Ng, C. A., Perry, M. D., Liang, W., Smith, N. J., Foo, B., Shrier, A., Lukacs, G. L., Hill, A. P., and Vandenberg, J. I. (2020) High-throughput phenotyping of heteromeric human ether-à-go-go-related gene potassium channel variants can discriminate pathogenic from rare benign variants. *Heart Rhythm* 17, 492-500
- 99. Jones, D. K., Liu, F., Dombrowski, N., Joshi, S., and Robertson, G. A. (2016) Dominant negative consequences of a hERG 1b-specific mutation associated with intrauterine fetal death. *Prog Biophys Mol Biol* **120**, 67-76
- 100. Jenewein, T., Kanner, S. A., Bauer, D., Hertel, B., Colecraft, H. M., Moroni, A., Thiel, G., and Kauferstein, S. (2020) The mutation L69P in the PAS domain of the hERG potassium channel results in LQTS by trafficking deficiency. *Channels (Austin)* 14, 163-174
- 101. Li, C. L., Hu, D. Y., Liu, W. L., Qi, S. Y., Wang, H. T., Li, L., Gong, Q. M., and Zhou, Z. F. (2007) [The mechanistic rote of KCNH2 gene L413P and L559H mutations in long QT syndrome]. *Zhonghua Nei Ke Za Zhi* 46, 838-841

- 102. Balijepalli, S. Y., Lim, E., Concannon, S. P., Chew, C. L., Holzem, K. E., Tester, D. J., Ackerman, M. J., Delisle, B. P., Balijepalli, R. C., and January, C. T. (2012) Mechanism of loss of Kv11.1 K+ current in mutant T421M-Kv11.1-expressing rat ventricular myocytes: interaction of trafficking and gating. *Circulation* 126, 2809-2818
- 103. Yang, H. T., Sun, C. F., Cui, C. C., Xue, X. L., Zhang, A. F., Li, H. B., Wang, D. Q., and Shu, J. (2009) HERG-F463L potassium channels linked to long QT syndrome reduce I(Kr) current by a trafficking-deficient mechanism. *Clin Exp Pharmacol Physiol* **36**, 822-827
- 104. Liu, L., Hayashi, K., Kaneda, T., Ino, H., Fujino, N., Uchiyama, K., Konno, T., Tsuda, T., Kawashiri, M. A., Ueda, K., Higashikata, T., Shuai, W., Kupershmidt, S., Higashida, H., and Yamagishi, M. (2013) A novel mutation in the transmembrane nonpore region of the KCNH2 gene causes severe clinical manifestations of long QT syndrome. *Heart Rhythm* 10, 61-67
- 105. Nakajima, T., Furukawa, T., Tanaka, T., Katayama, Y., Nagai, R., Nakamura, Y., and Hiraoka, M. (1998) Novel mechanism of HERG current suppression in LQT2: shift in voltage dependence of HERG inactivation. *Circ Res* **83**, 415-422
- 106. Kinoshita, K., Yamaguchi, Y., Nishide, K., Kimoto, K., Nonobe, Y., Fujita, A., Asano, K., Tabata, T., Mori, H., Inoue, H., Hata, Y., Fukurotani, K., and Nishida, N. (2012) A novel missense mutation causing a G487R substitution in the S2-S3 loop of human ether-à-go-go-related gene channel. *J Cardiovasc Electrophysiol* 23, 1246-1253
- 107. Amin, A. S., Herfst, L. J., Delisle, B. P., Klemens, C. A., Rook, M. B., Bezzina, C. R., Underkofler, H. A., Holzem, K. M., Ruijter, J. M., Tan, H. L., January, C. T., and Wilde, A. A. (2008) Fever-induced QTc prolongation and ventricular arrhythmias in individuals with type 2 congenital long QT syndrome. *J Clin Invest* 118, 2552-2561
- 108. Sanguinetti, M. C., Curran, M. E., Spector, P. S., and Keating, M. T. (1996) Spectrum of HERG K+-channel dysfunction in an inherited cardiac arrhythmia. *Proc Natl Acad Sci U S A* **93**, 2208-2212
- 109. Keller, S. H., Platoshyn, O., and Yuan, J. X. (2005) Long QT syndrome-associated I593R mutation in HERG potassium channel activates ER stress pathways. *Cell Biochem Biophys* **43**, 365-377
- 110. Furutani, M., Trudeau, M. C., Hagiwara, N., Seki, A., Gong, Q., Zhou, Z., Imamura, S., Nagashima, H., Kasanuki, H., Takao, A., Momma, K., January, C. T., Robertson, G. A., and Matsuoka, R. (1999) Novel mechanism associated with an inherited cardiac arrhythmia: defective protein trafficking by the mutant HERG (G601S) potassium channel. *Circulation* **99**, 2290-2294
- 111. Stump, M. R., Gong, Q., and Zhou, Z. (2012) Isoform-specific dominant-negative effects associated with hERG1 G628S mutation in long QT syndrome. *PLoS One* 7, e42552
- 112. Mao, H., Lu, X., Karush, J. M., Huang, X., Yang, X., Ba, Y., Wang, Y., Liu, N., Zhou, J., and Lian, J. (2013) Pharmacologic Approach to Defective Protein Trafficking in the E637K-hERG Mutant with PD-118057 and Thapsigargin. *PLoS One* **8**, e65481
- 113. Mihic, A., Chauhan, V. S., Gao, X., Oudit, G. Y., and Tsushima, R. G. (2011) Trafficking defect and proteasomal degradation contribute to the phenotype of a novel KCNH2 long QT syndrome mutation. *PLoS One* **6**, e18273
- 114. Li, K., Jiang, Q., Bai, X., Yang, Y. F., Ruan, M. Y., and Cai, S. Q. (2017) Tetrameric Assembly of K(+) Channels Requires ER-Located Chaperone Proteins. *Mol Cell* **65**, 52-65

115. Graves, T. K., Patel, S., Dannies, P. S., and Hinkle, P. M. (2001) Misfolded growth hormone causes fragmentation of the Golgi apparatus and disrupts endoplasmic reticulum-to-Golgi traffic. *J Cell Sci* **114**, 3685-3694